

引用格式：杨钰清，高彭，张健，等，2024. 不同变质条件下变基性岩中磷灰石地球化学特征：以古元古代华北中部造山带为例 [J]. 地质力学学报，30 (6)：991–1011. DOI: [10.12090/j.issn.1006-6616.2024046](https://doi.org/10.12090/j.issn.1006-6616.2024046)

Citation: YANG Y Q, GAO P, ZHANG J, et al., 2024. Geochemical characteristics of apatite in metabasic rocks under different metamorphic conditions: a case study from the Paleoproterozoic Trans-North China Orogen [J]. Journal of Geomechanics, 30 (6)：991–1011. DOI: [10.12090/j.issn.1006-6616.2024046](https://doi.org/10.12090/j.issn.1006-6616.2024046)

## 不同变质条件下变基性岩中磷灰石地球化学特征：以古元古代华北中部造山带为例

杨钰清<sup>1</sup>，高彭<sup>2</sup>，张健<sup>3</sup>，刘晓光<sup>4</sup>，程昌泉<sup>1</sup>，尹常青<sup>1</sup>，钱加慧<sup>1</sup>  
YANG Yuqing<sup>1</sup>，GAO Peng<sup>2</sup>，ZHANG Jian<sup>3</sup>，LIU Xiaoguang<sup>4</sup>，CHENG Changquan<sup>1</sup>，YIN Changqing<sup>1</sup>，QIAN Jiahui<sup>1</sup>

1. 中山大学地球科学与工程学院，广东 珠海 519082；
  2. 中国科学院壳幔物质与环境重点实验室中国科学技术大学地球和空间科学学院，安徽 合肥 230026；
  3. 香港大学地球科学系，香港 999077；
  4. 海底科学与探测技术教育部重点实验室中国海洋大学海洋地球科学学院，山东 青岛 266100
1. *School of Earth Sciences and Engineering, Sun Yat-sen University, Zhuhai 519082, Guangdong, China;*  
2. *CAS Key Laboratory of Crust-Mantle Materials and Environments, School of Earth and Space Sciences, University of Science and Technology of China, Hefei 230026, Anhui, China;*  
3. *Department of Earth Sciences, The University of Hong Kong, Hong Kong 999077, China;*  
4. *Key Lab of Submarine Geosciences and Prospecting Techniques, and College of Marine Geosciences, Ocean University of China, Qingdao 266100, Shandong, China*

### Geochemical characteristics of apatite in metabasic rocks under different metamorphic conditions: a case study from the Paleoproterozoic Trans-North China Orogen

**Abstract:** [Objective] Apatite is a common accessory mineral that is widely distributed in various rock types. Its U-Pb age, trace elements (particularly REE, Th, U, and Sr), and Sr-Nd isotopic compositions provide important information on its chronology and magmatism. However, the geochemical behavior at different metamorphic levels during orogenesis remains unclear. As a typical continent-to-continent collisional orogenic belt in the Paleoproterozoic, the Trans-North China Orogen (TNCO) has recorded an integrated metamorphic sequence ranging from greenschist to amphibolite to granulite facies. Therefore, it is an ideal area to study the geochemical behavior of apatite during various grades of metamorphism involving the orogenic process. [Methods] In this study, we systematically collected metabasic samples of different metamorphic grades, including greenschist, amphibolite, and mafic granulite, in the Wutai-Hengshan area of the TNCO. We conducted detailed petrographic observations and geochemical analyses of apatite grains from metabasic rocks with different metamorphic grades. [Results] Our results showed that the apatite grains from the greenschist samples had both magmatic and metamorphic origins. The apatite grains in the amphibolite samples were mainly of metamorphic origin. In contrast, the grains from the granulite samples were closely related to crustal anatexis, exhibiting geochemical characteristics of magmatic-origin apatite. [Conclusion] This study shows that trace element variations in apatite can clearly reflect the influence of metamorphic grades, crustal anatexis, and coexisting rock-forming minerals with variations

基金项目：国家自然科学基金项目 (42025204)

This research is financially supported by the National Natural Science Foundation of China (Grant No. 42025204).

第一作者：杨钰清 (1999—)，女，在读硕士，主要从事构造地质学研究。Email: [623359651@qq.com](mailto:623359651@qq.com)

通讯作者：张健 (1978—)，男，教授，主要从事构造地质学和前寒武纪地质学研究。Email: [jian@hku.hk](mailto:jian@hku.hk)

收稿日期：2024-04-28；修回日期：2024-05-22；录用日期：2024-05-23；网络出版日期：2024-07-25；责任编辑：范二平

in temperature and pressure conditions during metamorphism. [Significance] The results of this study provide new constraints to our understanding of elemental migration and the geochemical balance within apatite during orogeny.

**Keywords:** North China Craton; Trans-North China Orogen; metabasic rocks; metamorphism; apatite; trace elements

**摘要:** 磷灰石是一种常见的副矿物, 在各种岩石类型中均有产出, 其 U-Pb 年龄、微量元素 (特别是 REE、Th、U 和 Sr 等) 和 Sr-Nd 同位素组成可提供重要的年代学和地球化学信息。目前对于其在造山过程中不同变质级别下的地球化学行为的研究并不清楚。作为古元古代典型的陆-陆碰撞造山带, 华北克拉通中部造山带记录了一套从绿片岩相、经角闪岩相至麻粒岩相的完整变质岩石组合, 因而是研究基性岩变质演化过程磷灰石地球化学属性的理想区域。文章在中部造山带的五台-恒山地区系统采集了绿片岩、斜长角闪岩和基性麻粒岩样品, 并对不同变质级别变基性岩中的磷灰石进行了详细的岩相学和微量元素研究。研究表明, 绿片岩样品中含有岩浆成因和变质成因 2 种类型的磷灰石, 斜长角闪岩样品中主要为变质成因磷灰石, 而基性麻粒岩样品中主要为深熔型磷灰石, 表现出岩浆成因磷灰石的微量元素特征, 可能结晶自深熔熔体。研究表明磷灰石的微量元素变化能够清晰地反映变质演化过程中随温压条件变化而出现的熔体和共存结晶矿物的影响, 为了解造山作用过程中的元素迁移和平衡提供了新的约束。

**关键词:** 华北克拉通; 中部造山带; 变基性岩; 变质作用; 磷灰石; 微量元素

**中图分类号:** P584; P588.3 **文献标识码:** A **文章编号:** 1006-6616(2024)06-0991-21

**DOI:** 10.12090/j.issn.1006-6616.2024046

## 0 引言

磷灰石是地球上已知类型最丰富、分布最广泛的磷酸盐矿物之一, 是全球磷循环研究的基础 (Filippelli, 2002; Piccoli and Candela, 2002), 对地质学相关研究具有重要意义。磷灰石在大多数火成岩、变质岩和沉积岩中以副矿物形式出现。磷灰石晶体为六方晶系结构, 这种结构为多种元素以类质同象的形式进入其晶体结构提供了良好条件 (Hughes and Rakovan, 2015)。尽管变质岩类型多样, 但作为重要副矿物的磷灰石在不同原岩类型、变质级别的变质岩中表现出不同的存在状态和地球化学特征, 是研究岩石变质作用过程中元素迁移和平衡的理想对象 (Hoskin et al., 2000; 邢凯等, 2021; Liu et al., 2023)。随着国内外学者对磷灰石研究的不断深入, 不同元素指示的地质意义在岩石学研究中的重要性日益提高, 尤其以微量元素 (Sr、Y、Mn、REE、U、Th 及 Pb 等) 和卤族元素 (F、Cl、Br 等) 为代表 (Pan et al., 2016; Zhang et al., 2021)。在岩浆演化过程中, 磷灰石的结晶可以贯穿始终, 因此能够完整地记录岩浆结晶的全过程, 也包含了热液阶段的演化信息 (刘景波等, 2013; Chen and Simonetti, 2013; Zafar et al., 2020; Feng and Zheng, 2023)。此外, 磷灰石的地球化学组成也可用于计算氧逸度 (Stokes et al., 2019; Tang et al., 2020; Hammerli et al., 2021)、地质定年 (Chew

and Spinkings, 2021) 以及碎屑物源示踪 (O'Sullivan et al., 2020; O'Sullivan and Chew, 2020) 等多个方面。相关学者根据磷灰石的微量元素组成, 将其分为 3 种主要成因类型: 岩浆成因、变质成因和沉积成因 (Spear and Pyle, 2002; Gall et al., 2017)。其组成差异主要体现在稀土元素配分特征、Sr 含量和 Eu 负异常程度等。影响这一差异的因素包括分配系数、熔体组成、氧逸度和其他矿物的结晶顺序 (主要是与磷灰石竞争相关微量元素的矿物, 如斜长石竞争 Sr 和 Eu) 等 (Webster and Piccoli, 2015; Stokes et al., 2019; 詹琼睿等, 2022; Tan et al., 2023)。碰撞造山带内通常发育有不同变质程度的变质岩, 随着温压条件的变化, 这些岩石会经历不同程度 (包括深熔作用) 的变质演化过程。作为重要副矿物的磷灰石能否为这一重要的变质作用过程提供新的地球化学约束, 目前尚缺乏系统性的研究。

为探讨这一问题, 选择华北克拉通中部造山带的五台-恒山地区作为研究区。该地区出露了古元古代中部造山带最完整的从低级到高级变质序列的岩石组合 (Zhang et al., 2006, 2007, 2015; Qian et al., 2013; Peng et al., 2017)。已有研究表明, 该地区岩石主体形成于 2.55~2.50 Ga, 但均经历了 ~1.85 Ga 的变质事件, 因而是研究磷灰石在同一时间不同变质级别变质作用中地球化学行为的良好对象 (Wang et al., 2004; Kröner et al., 2005a; Polat et al., 2005; Liu et al., 2006, 2020; Trap et al., 2007; Zhang et

al., 2012; Tang and Santosh, 2018; Gao and Santosh, 2019; Gao et al., 2021)。根据已有研究报道的定年位置, 系统采集了绿片岩、斜长角闪岩和基性麻粒岩样品, 分别代表了在古元古代同一造山事件中的低级、中级和高级变质条件下的岩石组合, 并对不同变质级别变基性岩样品中的磷灰石进行了详细的岩相学和微量元素地球化学研究。研究结果将有助于对其成因类型进行区分, 从而对变质过程中熔体和其他结晶矿物的相互关系以及元素迁移和平衡进行综合约束。

## 1 地质背景及采样

华北克拉通是世界上重要的太古宙克拉通之

一, 面积约为  $150 \times 10^4 \text{ km}^2$ , 具有 38 亿年的地质演化历史, 经历了广泛的岩浆作用和高级变质作用 (Zhao et al., 2001, 2005; Zhai et al., 2005; Zhai and Santosh, 2011; Yang and Santosh, 2017; 翟明国, 2019; 万渝生等, 2022)。相关学者将华北克拉通的基底分为东部陆块和西部陆块, 两者被一个古元古代碰撞造山带分隔开, 称为中部造山带 (Trans-North China Orogen, TNCO; 图 1; Zhao et al., 1998, 2005, 2010, 2012; Yang and Santosh, 2015)。东部陆块和西部陆块在  $\sim 1.85 \text{ Ga}$  沿中部造山带发生碰撞, 基底岩石 (如 TTG、高压麻粒岩等) 记录了顺时针方向的压力-温度 ( $p$ - $T$ ) 路径, 表明中部造山带经历了古元古代的碰撞造山事件 (Zhao et al., 2000, 2001, 2005; Chen et al., 2020; Liu et al., 2020; Mao et al., 2024)。

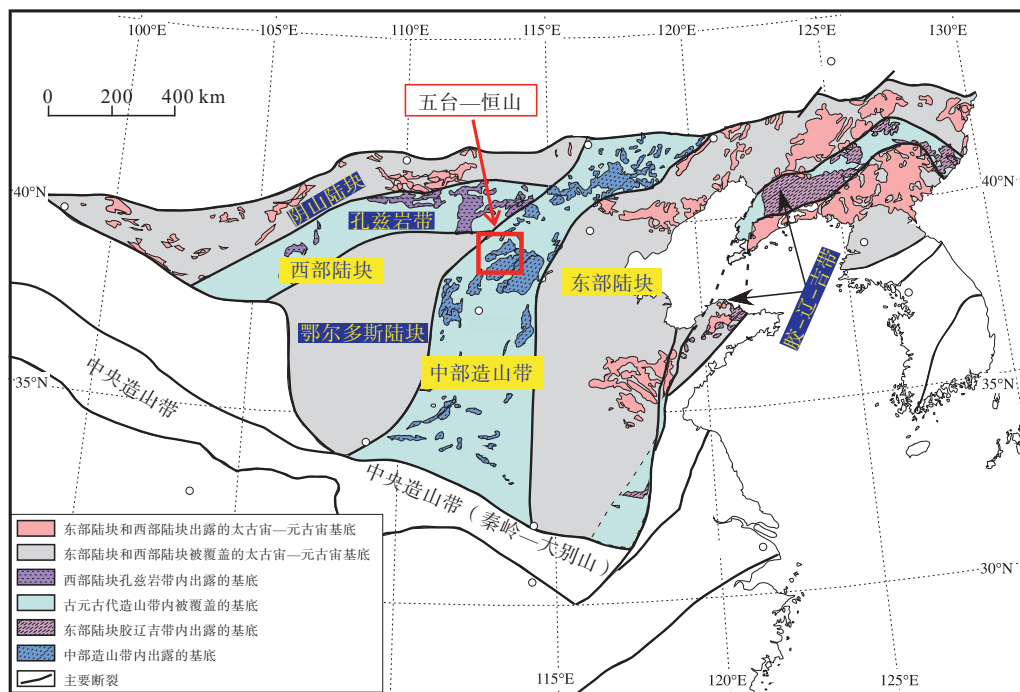


图 1 华北克拉通构造单元划分 (据 Zhao et al., 2001, 2005 修改)

Fig. 1 Tectonic subdivision of the North China Craton (modified after Zhao et al., 2001, 2005)

研究区位于中部造山带五台-恒山地区, 东南部的五台地区主要由中低级的花岗绿岩地体 (五台杂岩) 组成, 变质级别为绿片岩相和角闪岩相 (图 2, Zhang et al., 2006, 2015); 西北部的恒山地区则主要由高级片麻岩地体 (恒山杂岩) 组成, 恒山杂岩被东西向朱家坊韧性剪切带所分隔, 分为南、北 2 个部分 (图 2; Zhang et al., 2007, 2012; He et al., 2021)。

### 1.1 五台地区

五台地区内前寒武纪地质记录主要由表壳岩

系和侵入岩组成。其中表壳岩系包括新太古界五台群和古元古界溱沱群 (王欣平, 2023), 侵入岩包含新太古代-古元古代花岗岩体和少量超基性-基性岩体 (Liu et al., 2004; Sun et al., 2019)。新太古界五台群自下而上可划分为石咀亚群、台怀亚群和高凡亚群 3 个单元 (图 2; 白瑾, 1986; Zhang et al., 2012)。

下五台石咀亚群为角闪岩相变质的沉积-火山岩系, 由变橄榄岩、拉斑玄武岩、英安岩、砂岩和少

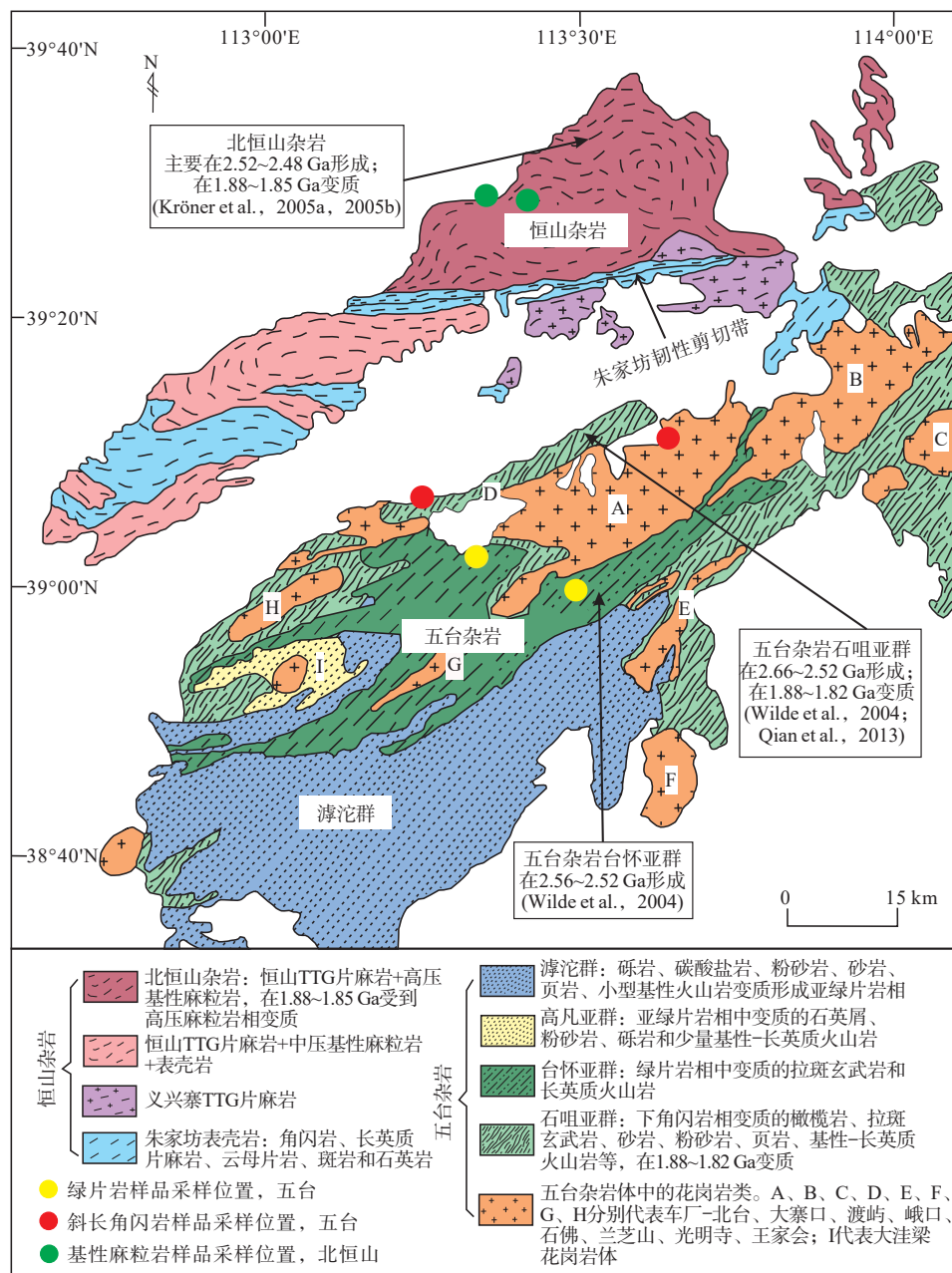


图2 五台杂岩和恒山杂岩主要岩性单元划分以及样品采集位置 (据 Zhao et al., 2007; Zhang et al., 2012 修改)

Fig. 2 Lithologic map of the Wutai-Hengshan Complex and the sampling locations in this study (modified after Zhao et al., 2007; Zhang et al., 2012)

量灰岩等组成。石咀亚群中发育有2.66~2.64 Ga的酸性火山岩、~2.50 Ga的基性火山岩和~2.52 Ga的中性火山岩，形成时代为新太古代晚期 (Wilde et al., 2004; Polat et al., 2005; Zhang et al., 2012; Wang et al., 2014)。

中五台台怀亚群分布在中部，是一套以绿片岩相为主的变火山岩组合，由长英质火山岩、枕状拉斑玄武岩和少量碎屑变质沉积岩组成，偶而有大理岩、石英岩夹层，构成一个完整的火山旋回。台怀亚群中发育有~2.54 Ga的安山岩和2.56~2.52 Ga

的酸性火山岩，指示台怀亚群形成于新太古代晚期 (Wilde et al., 2004; Liu et al., 2016b; Gao and Santosh, 2019)。

上五台高凡亚群以角度不整合覆盖在石咀亚群和台怀亚群之上，由石英岩、粉砂岩、砂岩、千枚岩和少量基性-长英质火山岩组成，变质程度为绿片岩相。最年轻的~2.35 Ga碎屑锆石年龄、~2.19 Ga的凝灰岩和~2.18 Ga的花岗侵入岩共同制约了高凡亚群的沉积时代为2.35~2.18 Ga (Zhang et al., 2012; Liu et al., 2016a; Peng et al., 2017)。

五台群中石咀亚群的变质程度最高,达到了高角闪岩相。基于变质程度的差异,过去的研究主要聚焦于石咀亚群的变质作用特征(魏春景,2018;赵远方等,2019)。对新太古界五台群石咀亚群变质作用的研究认为角闪岩相变质作用峰期可能发生在1.88~1.82 Ga(Kröner et al., 2005a; Liu et al., 2006; Trap et al., 2007; Qian et al., 2013; Qian and Wei, 2016)。

## 1.2 恒山地区

恒山地区主要由新太古代高级片麻岩和变质表壳岩组成,以朱家坊韧性剪切带为界可进一步划分为北恒山杂岩和南恒山杂岩2个部分(图2; Qian and Wei, 2016; Sun et al., 2019; He et al., 2021)。

北恒山杂岩主要由TTG片麻岩和高压基性麻粒岩组成,有许多高压基性颗粒在TTG片麻岩中呈布丁状或透镜体出现。其中侵位年龄在2.52~2.48 Ga的TTG片麻岩构成了花岗质片麻岩的主要组成部分(Kröner et al., 2005a),此外还有少量年龄为2.71~2.67 Ga的花岗质片麻岩,以及年龄分布在2.44~2.43 Ga和2.14~2.03 Ga的二长花岗质片麻岩(Liu et al., 2002, 2004; Kröner et al., 2005a, 2005b; Hu et al., 2021)。这些岩石普遍经历了部分熔融过程,并在1.88~1.85 Ga期间受到了高压麻粒岩相变质作用,并伴随着与造山作用相关的多期变形记录(Kröner et al., 2005a; 高山松等, 2023)。该地区与五台地区岩石组合在1.88~1.82 Ga期间共同经历了绿片岩相—角闪岩相—麻粒岩相变质作用(Liu et al., 2006; Trap et al., 2007)。

南恒山杂岩出露TTG片麻岩、中压基性麻粒岩和表壳岩以及义兴寨TTG片麻岩。恒山TTG片麻岩主要为层状正片麻岩,占杂岩的80%以上,这些岩石经历了1.90~1.85 Ga麻粒岩相变质作用和广泛的混合岩化作用(Zhang et al., 2007)。

朱家坊韧性剪切带位于南北恒山杂岩之间,近东西向,宽约2 km。朱家坊韧性剪切带主要发育义兴寨TTG片麻岩和变质表壳岩系,其主要岩石组合有角闪岩、长英质片麻岩、斑岩和石英岩等(Zhang et al., 2007; He et al., 2021)。He et al.(2021)曾对朱家坊韧性剪切带内的副片麻岩和花岗岩脉体进行定年,获得了 $1938\pm 31$  Ma的变质年龄和 $1860\pm 16$  Ma的花岗质脉体结晶年龄。

## 1.3 样品采集

五台—恒山地区的基性岩普遍经历了古元古

代的变质作用,包含绿片岩相—角闪岩相—麻粒岩相—整套从低级到高级的变质序列,因此成为研究变基性岩变质演化过程的理想地区。在该地区分别采集了具有代表性的变基性岩,采样位置见图2。在五台地区采集绿片岩、斜长角闪岩样品各2件,在恒山地区采集基性麻粒岩样品2件,共计6件样品。

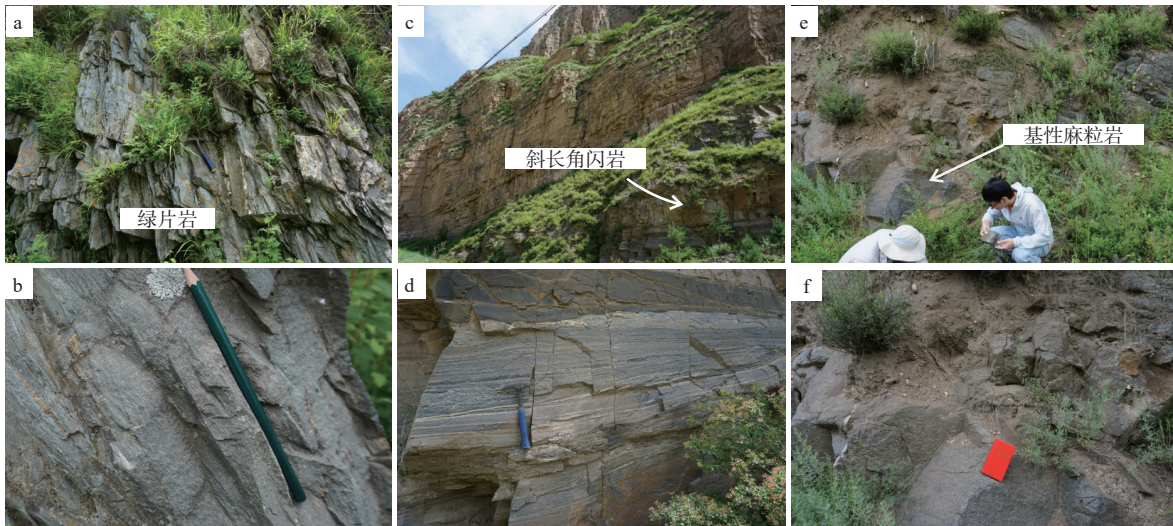
绿片岩样品22WT-03、22WT-21取自五台杂岩台怀亚群中,主体为钠长石绿泥石英片岩,绿片岩相变质,发育透入性片理,走向近北东—南西向,倾向北西向(图3a、3b)。斜长角闪岩样品22WT-07、22WT-22取自五台杂岩石咀亚群中,野外往往与变泥质岩、长英质片麻岩以条带状互层产出,中高角度、倾向南东向,部分以透镜体产出于长英质片麻岩中,具有和围岩相似的透入性片麻理(图3c、3d)。基性麻粒岩样品22WT-09、22WT-12取自北恒山杂岩中,野外以透镜体产出于TTG片麻岩中,主体为块状构造(图3e、3f),局部发育透入性面理,具有典型的“白眼圈”结构,表明其经历了峰期变质后的减压过程(Zhang et al., 2006)。

## 1.4 样品岩相学特征

绿片岩样品22WT-03(图4a、4b)为粒状变晶结构,片状构造。主要矿物为石英(45%)和绿泥石(35%)、钠长石(15%)及少量辉石(5%)。其中磷灰石颗粒普遍较小(10~20  $\mu\text{m}$ ,个别颗粒约为100  $\mu\text{m}$ ;图4b),主要与石英、长石共生。绿片岩样品22WT-21(图4c、4d)为粒状变晶结构,主要矿物为石英(48%)和绿泥石(37%),含少量白云母以及少量锆石等副矿物(15%)。其中磷灰石颗粒普遍较小(10~50  $\mu\text{m}$ ),主要包裹于石英中或与石英共生。

斜长角闪岩样品22WT-07(图4e、4f)为粒状变晶结构,片麻状构造。主要矿物为角闪石(70%)、斜长石(20%)和石英(10%)。其中磷灰石颗粒较大(100~200  $\mu\text{m}$ ),主要呈粒状,部分呈长柱状,主要包裹于角闪石中,与石英共生或被石英包裹。斜长角闪岩样品22WT-22(图4g、4h)为粒状变晶结构,主要矿物为角闪石(70%)、斜长石(18%)、石英(10%)和暗色矿物(2%)。其中磷灰石颗粒偏小(20~50  $\mu\text{m}$ ),主要与角闪石共生。

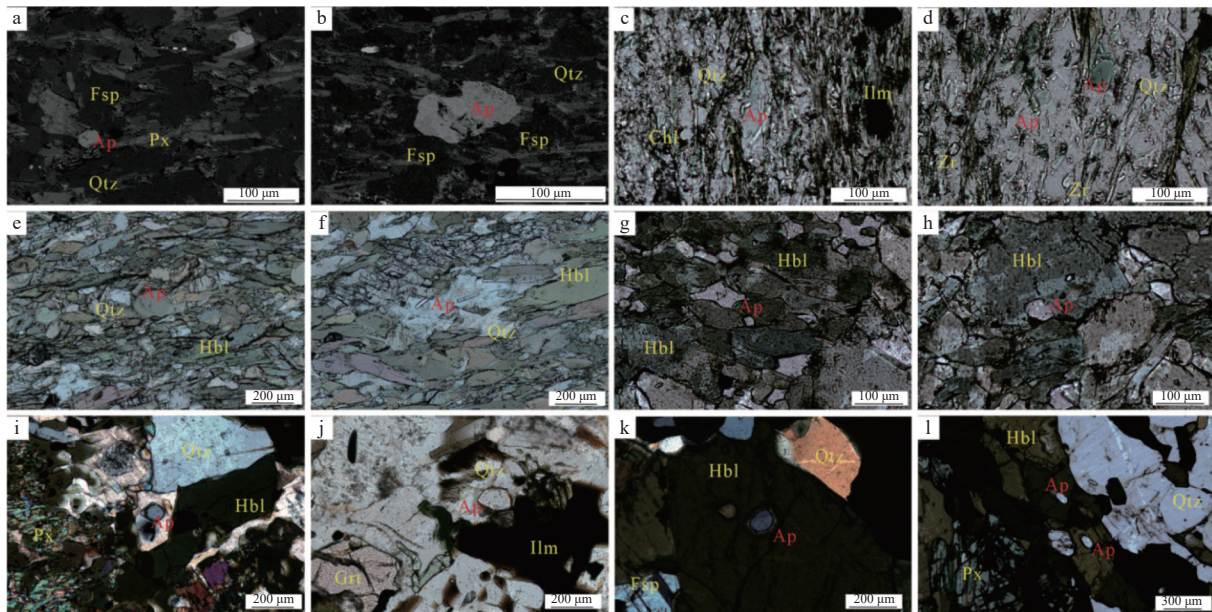
基性麻粒岩样品22WT-09(图4i、4j)为粒状变晶结构,块状构造。主要矿物为角闪石(30%)、石英(20%)、斜长石(20%)、辉石(15%)、石榴子石(10%)和钛铁矿等暗色矿物(5%)。其中磷灰石颗



a、b—绿片岩；c、d—斜长角闪岩；e、f—基性麻粒岩

图3 五台—恒山地区杂岩体中不同变质级别变基性岩野外照片和其对应的近照

Fig. 3 Field photograph of metabasic rocks of different metamorphic grades in the Wutai-Hengshan Complex and the representative photos (a, b) Greenschist; (c, d) Plagioclase amphibolite; (e, f) Mafic granulite



Ap—磷灰石；Chl—绿泥石；Fsp—长石；Grt—石榴子石；Hbl—角闪石；Ilm—钛铁矿；Px—辉石；Qtz—石英；Zr—锆石

a、b—22WT-03 样品；c、d—22WT-21 样品；e、f—22WT-07 样品；g、h—22WT-22 样品；i、j—22WT-09 样品；k、l—22WT-12 样品

图4 样品显微镜下特征

Fig. 4 Microscopic characteristics of the samples

(a, b) Sample 22WT-03; (c, d) Sample 22WT-21; (e, f) Sample 22WT-07; (g, h) Sample 22WT-22; (i, j) Sample 22WT-09; (k, l) Sample 22WT-12  
Ap—apatite; Chl—chlorite; Fsp—feldspar; Grt—garnet; Hbl—hornblende; Ilm—ilmenite; Px—pyroxene; Qtz—quartz; Zr—zircon

粒较大(100~200 μm), 主要被石英包裹。基性麻粒岩样品 22WT12(图 4k、4l), 主要矿物为角闪石(35%)、石英(25%)、辉石(20%)、斜长石(13%)和石榴子石(7%)。其中磷灰石颗粒较大(100~200 μm), 与角闪石共生或包裹在石英和角闪石中。

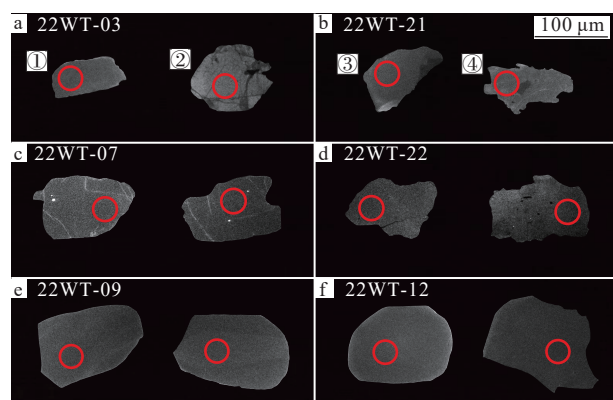
## 2 分析方法

### 2.1 样品前处理

样品前处理(切制薄片、磨粉及挑选单矿物等)

在武汉上谱分析技术有限公司完成。将挑选后的磷灰石固定在环氧树脂靶上进行抛光, 之后进行阴极发光 (CL) 图像拍摄。

绿片岩样品磷灰石颗粒在 CL 图中部分呈自形至半自形, 晶体形状较为完整, 成分结构较为均一 (图 5a①、5b③); 部分呈半自形至他形, 成分结构不均一, 边缘或整体存在裂隙 (图 5a②、5b④)。斜长角闪岩样品磷灰石颗粒在 CL 图中普遍呈半自形至他形, 有不规则分区, 成分结构不均一, 边缘或者整体存在裂隙 (图 5c、5d)。基性麻粒岩样品磷灰石颗粒在 CL 图中普遍呈自形至半自形, 晶体形状较为完整, 成分结构较为均一 (图 5e、5f)。



红圈为原位微量元素分析点, 束斑直径为 32 μm

a、b—绿片岩; c、d—斜长角闪岩; e、f—基性麻粒岩

图 5 代表性磷灰石 CL 图

Fig. 5 Cathodoluminescence (CL) images of the representative samples

(a, b) Greenschist; (c, d) Plagioclase amphibolite; (e, f) Mafic granulite

The red circle is the location of in-situ analysis, with a beam spot of 32 μm in width.

## 2.2 全岩主、微量元素

全岩主、微量元素在武汉上谱分析技术有限公司完成。使用日本 RIGAKU 公司生产的 Zsx Primus II 波长色散 X 射线荧光光谱仪 (XRF) 进行主量元素分析, 使用 Agilent 7700e ICP-MS 仪器进行微量元素分析。

## 2.3 磷灰石主量元素

磷灰石主量元素分析在南方海洋科学与工程广东实验室 (珠海) 海洋元素与同位素平台实验室完成, 使用仪器为配备有 4 道波谱仪的 JEOL JXA-iSP100 电子探针分析仪 (EPMA)。工作条件为加速电压 15 kV, 探针电流 10 nA 和束斑 10 μm。首先测量 K、Na、F、Cl 等活动性元素, 以减少分析过程中

的损失。使用 ZAF 校正程序对分析结果进行校正。用于校准的标准矿物如下: 正长石 (K)、磷灰石 (Ca 和 P)、钠长石 (Na 和 Al)、橄榄石 (Mg)、石英 (Si)、重晶石 (S)、萤石 (F)、硅铍铝钠石 (Cl)、磁铁矿 (Fe)、蔷薇辉石 (Mn) 和天青石 (Sr)。

## 2.4 磷灰石微量元素

磷灰石原位微量元素分析在中山大学海洋科学学院完成, 对 EPMA 测试的相同样品进行 LA-ICP-MS (激光剥蚀-电感耦合等离子体-质谱) 测试。分析使用相干 193 nm ArF 准分子激光烧蚀系统 (5 J/cm<sup>2</sup> 能量密度和 5 Hz 重复频率) 与 Agilent 7900 ICP-MS 联机。激光剥蚀坑直径为 32 μm, 深度为 10 μm。分析数据使用标准样品 NIST 612 (GeoRem 数据库) 进行校准, 并通过标样 NIST 610 进行监测。以平均 Ca 含量 (EPMA 分析结果) 作为内标。使用 Iolite 4 软件进行数据处理 (Paton et al., 2011)。

## 3 分析测试结果

### 3.1 全岩主、微量元素

五台—恒山地区 6 件变基性岩样品的全岩主、微量元素地球化学分析结果见表 1。经无水 100% 校正后, 变基性岩样品的 SiO<sub>2</sub> 含量为 44.7%~49.9%, 整体落在基性岩成分范围内, 以低 TiO<sub>2</sub> (0.60%~1.74%, <2%) 和低 MgO (3.57%~8.64%) 为特征 (表 1)。在 Nb/Y-Zr/Ti 图解 (图 6a) 中, 样品主要落在亚碱性玄武岩区域。同时根据 SiO<sub>2</sub>-TFeO/MgO 图解 (图 6b), 这些样品具有拉斑质特征, 这与样品的 TFeO/MgO 比值和 TiO<sub>2</sub> 含量呈正相关一致 (图 6c)。

同变质级别样品的球粒陨石标准化稀土元素配分曲线较为一致 (图 7a), 2 件斜长角闪岩样品之间略有差异, 表明其代表了不同的原岩成分。除斜长角闪岩样品 22WT-22 外, 大多数样品轻微富集轻稀土元素, 其 (La/Sm)<sub>N</sub> 比值为 1.32~3.08, (La/Yb)<sub>N</sub> 比值为 1.60~7.74, 绿片岩和基性麻粒岩样品具有轻微的 Eu 负异常 (δEu=0.83~0.90)。

在微量元素原始地幔标准化图中 (图 7b), 这些变基性岩明显亏损 Nb、Ta 和 Ti, 具有岛弧岩浆特征, Ce 和 Sm 显示出的轻微相对低值可能是由于两侧元素轻微富集造成的。绿片岩和斜长角闪岩亏损 P, 斜长角闪岩轻微亏损 Th, 基性麻粒岩亏损 Sr。

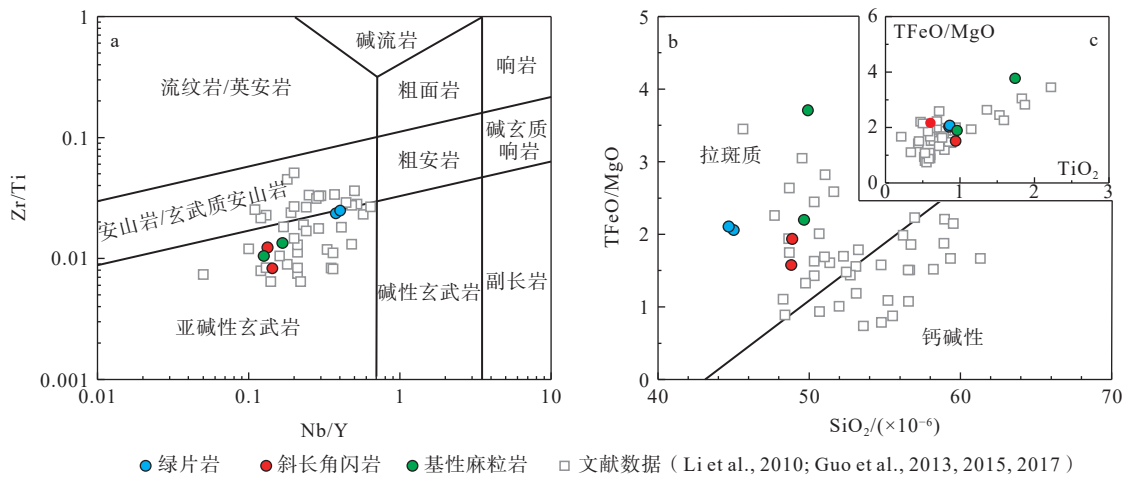
### 3.2 磷灰石主量元素

文章对五台—恒山地区采集的 6 件变基性岩

表 1 五台-恒山地区变基性岩全岩主量元素 (%) 与微量元素 ( $\times 10^{-6}$ ) 组成Table 1 Whole rock major (%) and trace element ( $\times 10^{-6}$ ) compositions of the metabasic rocks in the Wutai-Hengshan area

| 样品名称                            | 绿片岩     |         | 斜长角闪岩   |         | 基性麻粒岩    |         |
|---------------------------------|---------|---------|---------|---------|----------|---------|
|                                 | 22WT-03 | 22WT-21 | 22WT-07 | 22WT-22 | 22WT-09  | 22WT-12 |
| SiO <sub>2</sub>                | 44.98   | 44.66   | 49.63   | 48.79   | 49.89    | 48.85   |
| TiO <sub>2</sub>                | 0.85    | 0.86    | 0.60    | 0.94    | 1.74     | 0.96    |
| Al <sub>2</sub> O <sub>3</sub>  | 15.41   | 14.36   | 15.86   | 14.56   | 12.70    | 13.79   |
| TFe <sub>2</sub> O <sub>3</sub> | 8.46    | 8.38    | 11.31   | 12.71   | 18.70    | 14.98   |
| MnO                             | 0.16    | 0.18    | 0.15    | 0.17    | 0.26     | 0.22    |
| MgO                             | 3.69    | 3.57    | 7.64    | 7.22    | 4.54     | 6.95    |
| CaO                             | 12.58   | 11.02   | 9.60    | 11.36   | 9.31     | 10.82   |
| Na <sub>2</sub> O               | 1.32    | 1.08    | 1.79    | 1.75    | 2.31     | 1.75    |
| K <sub>2</sub> O                | 2.65    | 3.13    | 0.75    | 0.15    | 0.78     | 1.00    |
| P <sub>2</sub> O <sub>5</sub>   | 0.30    | 0.34    | 0.07    | 0.07    | 0.20     | 0.10    |
| LOI                             | 8.72    | 11.90   | 2.08    | 2.07    | -0.01    | 0.32    |
| SUM                             | 99.12   | 99.49   | 99.48   | 99.79   | 100.41   | 99.72   |
| FeO                             | 5.28    | 5.05    | 6.60    | 8.60    | 10.90    | 10.30   |
| TFeO                            | 7.61    | 7.55    | 9.28    | 11.44   | 16.83    | 13.48   |
| Sc                              | 12.47   | 22.45   | 35.43   | 40.88   | 43.82    | 46.57   |
| Ti                              | 5095.75 | 5167.69 | 3620.98 | 5605.33 | 10413.32 | 5725.23 |
| V                               | 95.41   | 174.57  | 213.12  | 284.21  | 356.60   | 297.35  |
| Cr                              | 124.66  | 501.90  | 134.69  | 184.70  | 29.56    | 77.51   |
| Co                              | 14.30   | 29.08   | 51.54   | 50.83   | 49.84    | 58.67   |
| Ni                              | 55.87   | 133.80  | 177.18  | 106.60  | 26.91    | 69.78   |
| Cu                              | 11.02   | 74.26   | 78.99   | 122.01  | 45.55    | 83.11   |
| Zn                              | 304.52  | 72.84   | 74.29   | 88.04   | 141.05   | 92.70   |
| Ga                              | 15.46   | 18.13   | 15.63   | 16.69   | 19.38    | 16.84   |
| Rb                              | 57.80   | 116.88  | 20.92   | 2.86    | 26.98    | 47.35   |
| Sr                              | 99.51   | 774.66  | 199.13  | 112.84  | 119.17   | 64.81   |
| Y                               | 13.38   | 24.35   | 14.14   | 18.32   | 44.90    | 24.79   |
| Zr                              | 121.28  | 130.53  | 44.74   | 46.49   | 138.71   | 60.03   |
| Nb                              | 5.04    | 9.80    | 1.88    | 2.62    | 7.51     | 3.12    |
| Sn                              | 0.94    | 1.36    | 0.51    | 0.47    | 1.27     | 0.61    |
| Cs                              | 0.61    | 1.42    | 2.45    | 0.38    | 0.60     | 0.51    |
| Ba                              | 311.93  | 1053.04 | 93.76   | 18.27   | 199.41   | 151.06  |
| La                              | 16.21   | 23.60   | 4.91    | 2.32    | 13.49    | 5.87    |
| Ce                              | 36.33   | 52.03   | 10.97   | 6.24    | 33.84    | 13.63   |
| Pr                              | 4.32    | 6.60    | 1.57    | 1.06    | 4.67     | 2.02    |
| Nd                              | 15.92   | 27.17   | 6.64    | 5.50    | 20.39    | 9.50    |
| Sm                              | 3.29    | 5.31    | 1.84    | 1.95    | 5.67     | 2.78    |
| Eu                              | 0.91    | 1.40    | 0.72    | 0.69    | 1.68     | 0.91    |
| Gd                              | 2.77    | 4.60    | 2.22    | 2.67    | 6.58     | 3.53    |
| Tb                              | 0.44    | 0.72    | 0.40    | 0.48    | 1.10     | 0.60    |
| Dy                              | 2.53    | 4.17    | 2.48    | 3.11    | 7.62     | 4.14    |
| Ho                              | 0.53    | 0.85    | 0.54    | 0.67    | 1.63     | 0.90    |
| Er                              | 1.41    | 2.37    | 1.54    | 1.98    | 4.78     | 2.46    |
| Tm                              | 0.21    | 0.35    | 0.22    | 0.28    | 0.66     | 0.36    |
| Yb                              | 1.42    | 2.34    | 1.53    | 1.92    | 4.61     | 2.48    |
| Lu                              | 0.21    | 0.36    | 0.22    | 0.29    | 0.69     | 0.38    |
| Hf                              | 3.14    | 3.13    | 1.26    | 1.29    | 3.75     | 1.66    |
| Ta                              | 0.38    | 0.47    | 0.11    | 0.15    | 0.47     | 0.18    |
| Pb                              | 4.95    | 8.84    | 2.03    | 0.98    | 2.66     | 0.90    |
| Th                              | 5.33    | 3.95    | 0.50    | 0.21    | 2.30     | 0.58    |
| U                               | 1.17    | 1.01    | 0.12    | 0.06    | 0.50     | 0.09    |
| (La/Sm) <sub>N</sub>            | 3.08    | 2.77    | 1.67    | 0.74    | 1.49     | 1.32    |
| (La/Yb) <sub>N</sub>            | 7.74    | 6.84    | 2.18    | 0.82    | 1.99     | 1.60    |
| δEu                             | 0.89    | 0.84    | 1.08    | 0.92    | 0.84     | 0.89    |

注: 部分样品的烧失量为负数, 因为样品中可能含有较多的低价态金属氧化物, 高温氧化, 所以烧失量为负数

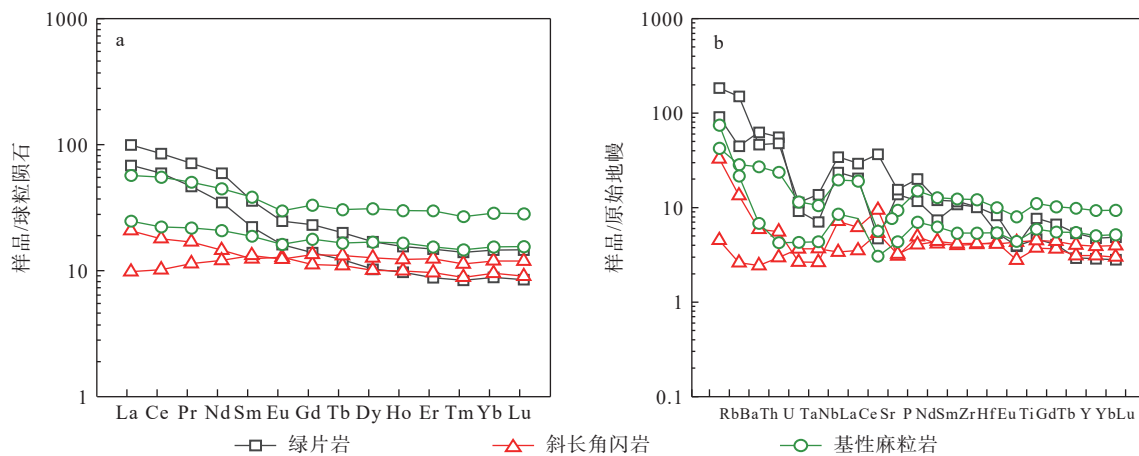


a—Nb/Y-Zr/Ti 图解 (底图据 Pearce, 1996); b—SiO<sub>2</sub>-TFeO/MgO 图解 (底图据 Miyashiro, 1974); c—TiO<sub>2</sub>-TFeO/MgO 图

图 6 五台—恒山地区变基性岩全岩主量元素图解

Fig. 6 Diagram of whole rock major element of the metabasic rocks in the Wutai-Hengshan area

(a) Nb/Y-Zr/Ti classification diagram of metabasic rocks in Wutai and Hengshan (modified after Pearce, 1996); (b) SiO<sub>2</sub>-TFeO/MgO classification diagram (modified after Miyashiro, 1974); (c) Diagram of TiO<sub>2</sub>-TFeO/MgO



a—变基性岩球粒陨石标准化稀土元素配分图; b—原始地幔标准化微量元素蛛网图

图 7 全岩微量元素图解 (标准化值据 Sun and McDonough, 1989)

Fig. 7 Diagram of whole rock trace element (standardized values according to Sun and McDonough, 1989)

(a) Chondrite-normalized diagram of rare earth element for the metabasic rocks; (b) Primitive mantle-normalized diagram of trace elements for the metabasic rocks

样品中的磷灰石进行了主、微量元素分析, 分析结果见表 2。磷灰石主量元素组成主要为 CaO、P<sub>2</sub>O<sub>5</sub> 和 F 等, 其中 CaO 含量最高 (54.0%~55.0%), P<sub>2</sub>O<sub>5</sub> 含量为 41.0%~42.4%, 不同变质级别样品的差距很小。F 含量为 1.24%~5.22%, 斜长角闪岩样品的 F 含量明显低于绿片岩和基性麻粒岩样品, 但 Cl 含量高于绿片岩和基性麻粒岩样品 (图 8a、8b, 表 2)。

绿片岩样品中的磷灰石 (编号 Ap-03 和 Ap-21) 主量元素特征如下: CaO 的变化范围为 53.9%~

55.0%, 平均为 54.5%; P<sub>2</sub>O<sub>5</sub> 的变化范围为 40.3%~42.9%, 平均为 41.9%; F 含量的变化范围为 4.07%~5.22%, 平均为 4.54%。斜长角闪岩样品中的磷灰石 (编号 Ap-07 和 Ap-22) 主量元素特征如下: CaO 的变化范围为 53.2%~55.2%, 平均为 54.4%; P<sub>2</sub>O<sub>5</sub> 的变化范围为 41.0%~42.6%, 平均为 41.9%; F 含量的变化范围为 1.24%~4.50%, 平均为 1.96%。基性麻粒岩样品中的磷灰石 (编号 Ap-09 和 Ap-12) 主量元素特征如下: CaO 的变化范围为 53.7%~55.1%, 平均为 54.4%;

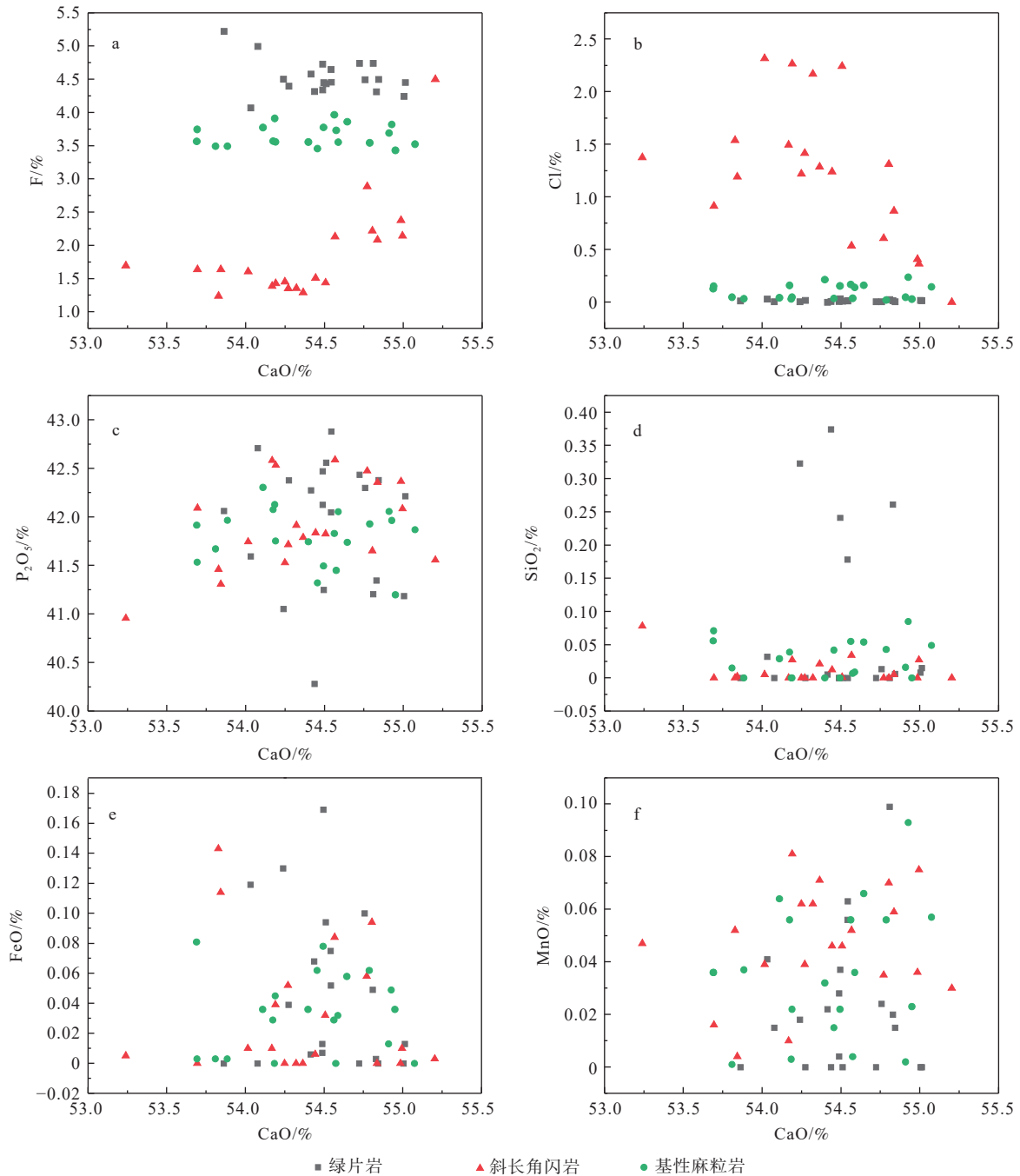
表 2 五台—恒山地区变基性岩磷灰石主量元素组成 (%)

Table 2 Apatite major element compositions of the metabasic rocks in the Wutai-Hengshan area (%)

| 样品点号     | K <sub>2</sub> O | SO <sub>3</sub> | CaO   | FeO  | MgO  | Al <sub>2</sub> O <sub>3</sub> | P <sub>2</sub> O <sub>5</sub> | SrO  | MnO  | Na <sub>2</sub> O | SiO <sub>2</sub> | F    | Cl   | 合计     |
|----------|------------------|-----------------|-------|------|------|--------------------------------|-------------------------------|------|------|-------------------|------------------|------|------|--------|
| Ap-03-1  | 0                | 0.12            | 54.83 | 0    | 0    | 0                              | 41.34                         | 0.03 | 0.02 | 0.05              | 0.26             | 4.31 | 0.02 | 99.17  |
| Ap-03-2  | 0                | 0.06            | 55.00 | 0    | 0    | 0.02                           | 41.18                         | 0.08 | 0    | 0                 | 0.01             | 4.24 | 0.02 | 98.83  |
| Ap-03-3  | 0                | 0.12            | 54.03 | 0.12 | 0.02 | 0                              | 41.59                         | 0.07 | 0.04 | 0.03              | 0.03             | 4.07 | 0.03 | 98.44  |
| Ap-03-4  | 0                | 0               | 54.49 | 0.01 | 0    | 0.03                           | 42.13                         | 0.10 | 0.03 | 0                 | 0                | 4.73 | 0.02 | 99.52  |
| Ap-03-5  | 0                | 0.26            | 54.54 | 0.08 | 0    | 0                              | 42.05                         | 0.14 | 0.06 | 0.06              | 0.18             | 4.65 | 0.02 | 100.07 |
| Ap-03-6  | 0                | 0               | 54.81 | 0.05 | 0    | 0                              | 41.21                         | 0.03 | 0.10 | 0.06              | 0                | 4.74 | 0.03 | 99.02  |
| Ap-03-7  | 0                | 0.16            | 54.24 | 0.13 | 0    | 0                              | 41.05                         | 0.04 | 0.02 | 0.04              | 0.32             | 4.50 | 0    | 98.62  |
| Ap-03-8  | 0                | 0.32            | 54.44 | 0.07 | 0.01 | 0.02                           | 40.28                         | 0.16 | 0    | 0.06              | 0.37             | 4.32 | 0.01 | 98.23  |
| Ap-03-9  | 0.02             | 0.24            | 54.50 | 0.17 | 0.13 | 0                              | 41.25                         | 0.19 | 0.04 | 0.11              | 0.24             | 4.45 | 0.03 | 99.47  |
| Ap-03-10 | 0                | 0.07            | 54.49 | 0.01 | 0.01 | 0.02                           | 42.47                         | 0.05 | 0    | 0.08              | 0                | 4.34 | 0.01 | 99.72  |
| Ap-21-1  | 0                | 0.01            | 54.54 | 0.05 | 0    | 0                              | 42.88                         | 0.35 | 0.06 | 0                 | 0                | 4.46 | 0.01 | 100.49 |
| Ap-21-2  | 0                | 0               | 54.84 | 0    | 0    | 0.01                           | 42.38                         | 0.34 | 0.02 | 0                 | 0.01             | 4.50 | 0    | 100.20 |
| Ap-21-3  | 0                | 0.01            | 55.01 | 0.01 | 0    | 0.01                           | 42.21                         | 0.34 | 0    | 0                 | 0.02             | 4.45 | 0.01 | 100.20 |
| Ap-21-4  | 0.01             | 0               | 53.86 | 0    | 0    | 0.01                           | 42.06                         | 0.40 | 0    | 0.01              | 0                | 5.22 | 0.01 | 99.38  |
| Ap-21-5  | 0.02             | 0.01            | 54.42 | 0.01 | 0    | 0                              | 42.27                         | 0.43 | 0.02 | 0                 | 0.01             | 4.58 | 0    | 99.84  |
| Ap-21-6  | 0.01             | 0               | 54.76 | 0.10 | 0    | 0                              | 42.30                         | 0.38 | 0.02 | 0.01              | 0.01             | 4.49 | 0    | 100.20 |
| Ap-21-7  | 0                | 0               | 54.27 | 0.04 | 0    | 0                              | 42.38                         | 0.32 | 0    | 0                 | 0                | 4.40 | 0.02 | 99.57  |
| Ap-21-8  | 0.02             | 0.02            | 54.08 | 0    | 0    | 0                              | 42.71                         | 0.17 | 0.02 | 0                 | 0                | 5.00 | 0    | 99.90  |
| Ap-21-9  | 0                | 0.01            | 54.51 | 0.09 | 0.02 | 0.01                           | 42.56                         | 0.36 | 0    | 0                 | 0                | 4.43 | 0.01 | 100.14 |
| Ap-21-10 | 0                | 0.03            | 54.72 | 0    | 0.01 | 0.02                           | 42.44                         | 0.36 | 0    | 0                 | 0                | 4.74 | 0.01 | 100.33 |
| Ap-07-1  | 0.01             | 0.05            | 55.20 | 0    | 0    | 0.02                           | 41.56                         | 0.10 | 0.03 | 0.03              | 0                | 4.50 | 0    | 99.62  |
| Ap-07-2  | 0.03             | 0               | 53.24 | 0.01 | 0.36 | 0.38                           | 40.96                         | 0.02 | 0.05 | 0.02              | 0.08             | 1.70 | 1.38 | 98.18  |
| Ap-07-3  | 0                | 0.02            | 54.37 | 0    | 0    | 0                              | 41.79                         | 0.02 | 0.07 | 0.01              | 0.02             | 1.29 | 1.28 | 98.04  |
| Ap-07-4  | 0.01             | 0               | 54.27 | 0.05 | 0    | 0                              | 41.72                         | 0.01 | 0.04 | 0.03              | 0                | 1.35 | 1.42 | 98.01  |
| Ap-07-5  | 0                | 0               | 54.25 | 0    | 0.03 | 0                              | 41.53                         | 0.04 | 0.06 | 0                 | 0                | 1.45 | 1.22 | 97.69  |
| Ap-07-6  | 0.01             | 0.08            | 54.44 | 0.01 | 0.01 | 0                              | 41.84                         | 0.03 | 0.05 | 0                 | 0.01             | 1.51 | 1.24 | 98.30  |
| Ap-07-7  | 0.03             | 0               | 53.83 | 0.14 | 0    | 0                              | 41.46                         | 0.04 | 0.05 | 0.01              | 0                | 1.24 | 1.54 | 97.46  |
| Ap-07-8  | 0                | 0.03            | 53.70 | 0    | 0.01 | 0                              | 42.09                         | 0    | 0.02 | 0.02              | 0                | 1.64 | 0.91 | 97.51  |
| Ap-07-9  | 0                | 0               | 54.17 | 0.01 | 0.02 | 0                              | 42.58                         | 0.01 | 0.01 | 0.04              | 0                | 1.39 | 1.49 | 98.80  |
| Ap-07-10 | 0.01             | 0.03            | 53.84 | 0.11 | 0    | 0                              | 41.31                         | 0.01 | 0    | 0                 | 0                | 1.64 | 1.19 | 97.19  |
| Ap-22-1  | 0                | 0.03            | 54.19 | 0.04 | 0    | 0                              | 42.53                         | 0.01 | 0.08 | 0.04              | 0.03             | 1.43 | 2.27 | 99.53  |
| Ap-22-2  | 0                | 0.07            | 54.51 | 0.03 | 0    | 0                              | 41.83                         | 0.01 | 0.05 | 0.07              | 0                | 1.44 | 2.24 | 99.13  |
| Ap-22-3  | 0.01             | 0.03            | 54.84 | 0    | 0.04 | 0                              | 42.35                         | 0    | 0.06 | 0                 | 0.01             | 2.08 | 0.87 | 99.20  |
| Ap-22-4  | 0.01             | 0               | 54.99 | 0    | 0    | 0.01                           | 42.37                         | 0.03 | 0.04 | 0                 | 0                | 2.38 | 0.41 | 99.13  |
| Ap-22-5  | 0                | 0.02            | 54.57 | 0.08 | 0    | 0                              | 42.59                         | 0.02 | 0.05 | 0                 | 0.03             | 2.13 | 0.54 | 99.01  |
| Ap-22-6  | 0                | 0               | 54.02 | 0.01 | 0    | 0.01                           | 41.74                         | 0.02 | 0.04 | 0.02              | 0.01             | 1.61 | 2.32 | 98.58  |
| Ap-22-7  | 0                | 0.02            | 54.80 | 0.09 | 0    | 0                              | 41.65                         | 0.04 | 0.07 | 0                 | 0                | 2.22 | 1.31 | 98.98  |
| Ap-22-8  | 0                | 0.04            | 54.77 | 0.06 | 0.01 | 0.02                           | 42.47                         | 0.01 | 0.04 | 0                 | 0                | 2.89 | 0.61 | 99.56  |
| Ap-22-9  | 0                | 0.01            | 54.32 | 0    | 0    | 0                              | 41.91                         | 0.01 | 0.06 | 0                 | 0                | 1.35 | 2.17 | 98.78  |
| Ap-22-10 | 0.01             | 0               | 55.00 | 0.01 | 0.03 | 0                              | 42.08                         | 0    | 0.08 | 0                 | 0.03             | 2.14 | 0.37 | 98.75  |
| Ap-09-1  | 0                | 0               | 54.95 | 0.04 | 0.01 | 0                              | 41.20                         | 0.02 | 0.02 | 0.01              | 0                | 3.43 | 0.03 | 98.26  |
| Ap-09-2  | 0                | 0.03            | 54.18 | 0    | 0.02 | 0                              | 42.13                         | 0.01 | 0    | 0.01              | 0                | 3.91 | 0.03 | 98.67  |
| Ap-09-3  | 0                | 0               | 54.45 | 0.06 | 0.01 | 0                              | 41.32                         | 0    | 0.02 | 0                 | 0.04             | 3.46 | 0.04 | 97.93  |
| Ap-09-4  | 0                | 0.02            | 53.81 | 0    | 0    | 0.01                           | 41.67                         | 0    | 0    | 0.01              | 0.02             | 3.49 | 0.05 | 97.60  |
| Ap-09-5  | 0.01             | 0               | 54.91 | 0.01 | 0.01 | 0                              | 42.06                         | 0.02 | 0    | 0.02              | 0.02             | 3.69 | 0.05 | 99.23  |
| Ap-09-6  | 0                | 0               | 54.79 | 0.06 | 0    | 0                              | 41.93                         | 0.01 | 0.06 | 0                 | 0.04             | 3.54 | 0.02 | 98.96  |
| Ap-09-7  | 0                | 0.03            | 54.57 | 0    | 0.02 | 0.02                           | 41.45                         | 0    | 0    | 0.03              | 0.01             | 3.73 | 0.04 | 98.32  |
| Ap-09-8  | 0                | 0.05            | 53.88 | 0    | 0    | 0.01                           | 41.97                         | 0    | 0.04 | 0                 | 0                | 3.49 | 0.03 | 98.00  |
| Ap-09-9  | 0                | 0               | 54.11 | 0.04 | 0.02 | 0                              | 42.30                         | 0    | 0.06 | 0.04              | 0.03             | 3.78 | 0.04 | 98.83  |
| Ap-09-10 | 0                | 0.01            | 54.19 | 0.05 | 0    | 0                              | 41.75                         | 0    | 0.02 | 0.04              | 0                | 3.56 | 0.05 | 98.15  |
| Ap-12-1  | 0                | 0               | 54.49 | 0.08 | 0    | 0                              | 41.50                         | 0.02 | 0.02 | 0.09              | 0                | 3.78 | 0.15 | 98.51  |
| Ap-12-2  | 0                | 0.06            | 54.59 | 0.03 | 0    | 0.02                           | 42.05                         | 0.02 | 0.04 | 0.01              | 0.01             | 3.56 | 0.14 | 99.00  |
| Ap-12-3  | 0                | 0               | 53.69 | 0    | 0    | 0.01                           | 41.54                         | 0.02 | 0.04 | 0                 | 0.07             | 3.75 | 0.15 | 97.65  |
| Ap-12-4  | 0.01             | 0.04            | 54.56 | 0.03 | 0    | 0                              | 41.83                         | 0.03 | 0.06 | 0                 | 0.06             | 3.97 | 0.17 | 99.04  |
| Ap-12-5  | 0                | 0               | 54.17 | 0.03 | 0.01 | 0                              | 42.08                         | 0.01 | 0.06 | 0.04              | 0.04             | 3.57 | 0.16 | 98.62  |

续表 2

| 样品点号     | K <sub>2</sub> O | SO <sub>3</sub> | CaO   | FeO  | MgO | Al <sub>2</sub> O <sub>3</sub> | P <sub>2</sub> O <sub>5</sub> | SrO  | MnO  | Na <sub>2</sub> O | SiO <sub>2</sub> | F    | Cl   | 合计    |
|----------|------------------|-----------------|-------|------|-----|--------------------------------|-------------------------------|------|------|-------------------|------------------|------|------|-------|
| Ap-12-6  | 0                | 0.04            | 55.07 | 0    | 0   | 0.01                           | 41.87                         | 0    | 0.06 | 0.04              | 0.05             | 3.52 | 0.15 | 99.30 |
| Ap-12-7  | 0.03             | 0.01            | 53.69 | 0.08 | 0   | 0                              | 41.92                         | 0    | 0.04 | 0.05              | 0.06             | 3.57 | 0.13 | 98.03 |
| Ap-12-8  | 0.03             | 0.02            | 54.64 | 0.06 | 0   | 0.04                           | 41.74                         | 0    | 0.07 | 0.03              | 0.05             | 3.86 | 0.16 | 99.05 |
| Ap-12-9  | 0                | 0               | 54.93 | 0.05 | 0   | 0                              | 41.96                         | 0    | 0.09 | 0                 | 0.09             | 3.82 | 0.24 | 99.52 |
| Ap-12-10 | 0                | 0.01            | 54.40 | 0.04 | 0   | 0.01                           | 41.75                         | 0.03 | 0.03 | 0.01              | 0                | 3.56 | 0.22 | 98.49 |



a—F—CaO 图解; b—Cl—CaO 图解; c—P<sub>2</sub>O<sub>5</sub>—CaO 图解; d—SiO<sub>2</sub>—CaO 图解; e—FeO—CaO 图解; f—MnO—CaO 图解

图 8 不同变质级别样品中磷灰石主量元素图解

Fig. 8 Major element diagram of apatite grains of different metamorphic grades

(a) F—CaO relationship diagram; (b) Cl—CaO relationship diagram; (c) P<sub>2</sub>O<sub>5</sub>—CaO relationship diagram; (d) SiO<sub>2</sub>—CaO relationship diagram; (e) FeO—CaO relationship diagram; (f) MnO—CaO relationship diagram

$P_2O_5$  的变化范围为 41.2%~42.3%，平均为 41.8%；F 含量的变化范围为 3.43%~3.97%，平均为 3.66%。

综合来看，不同变质级别变基性岩样品中的磷灰石主量元素区别主要为卤族元素，CaO 和  $P_2O_5$  含量在不同变质级别样品中并无显著区别(图 8, 表 2)。

### 3.3 磷灰石微量元素

变基性岩样品中磷灰石的微量元素组成特征各异，但整体亏损大离子亲石元素(如 Rb; 表 3, 表 4)。绿片岩和斜长角闪岩样品具有轻微 Eu 负异常，基性麻粒岩样品具有明显 Eu 负异常。不同样品 REE 含量差别较大，斜长角闪岩样品 REE 含量明显低于绿片岩和基性麻粒岩样品(图 9)。

绿片岩样品中磷灰石  $\Sigma$ REE 含量分布在  $(120 \sim 7488) \times 10^{-6}$ ，平均为  $1728 \times 10^{-6}$ ，变化范围较大。Sr 含量分布在  $(368 \sim 357) \times 10^{-6}$ ，平均为  $1521 \times 10^{-6}$ ，部分具有 Sr 负异常。斜长角闪岩样品  $\Sigma$ REE 含量分布在  $(1.04 \sim 189) \times 10^{-6}$ ，平均为  $92 \times 10^{-6}$ ，整体含量较低。Sr 含量分布在  $(161 \sim 441) \times 10^{-6}$ ，平均为  $246 \times 10^{-6}$ ，低于绿片岩样品，部分具有 Sr 负异常。基性麻粒岩样品  $\Sigma$ REE 含量分布在  $(442 \sim 2056) \times 10^{-6}$ ，平均为  $1033 \times 10^{-6}$ 。Sr 含量分布在  $(76 \sim 261) \times 10^{-6}$ ，平均为  $155 \times 10^{-6}$ ，低于绿片岩，与斜长角闪岩样品相近，全部存在 Sr 负异常。

## 4 讨论

### 4.1 变基性岩中磷灰石的成因类型

O'Sullivan et al. (2020) 针对不同变质级别和不同原岩类型样品中磷灰石的微量元素组成进行研究，据此区分出不同成因类型的磷灰石(图 10)。此研究所使用样品均为变基性岩，其原岩属于岩浆岩，因而不存在沉积成因磷灰石，主要存在岩浆成因和变质成因 2 种类型。相比变质成因磷灰石，岩浆成因磷灰石的轻稀土元素富集程度更高，微量元素含量从 LREE 至 HREE 整体呈缓慢下降趋势，而变质成因磷灰石并不存在这一特点。同时，岩浆成因磷灰石具有显著的 Sr 负异常与 Eu 负异常，而变质成因磷灰石则包括 Sr 与 Eu 的正异常与负异常 2 种情况，但整体而言，岩浆成因磷灰石表现比变质成因磷灰石更高的 Sr 负异常和轻稀土富集程度。

根据 O'Sullivan et al. (2020) 的划分依据，可将文中磷灰石样品进行如下划分：①在低级变质阶段，绿片岩样品 22WT-03 和 22WT-21 轻稀土元素变化

范围非常广，其中可能存在岩浆成因和变质成因 2 种类型的磷灰石。岩浆成因磷灰石表现出明显的轻稀土元素富集(如 La、Ce 等)， $(La/Yb)_N$  比值为 1.37~39.97，平均为 16.25；具有 Eu 负异常( $\delta Eu = 0.51 \sim 0.83$ )，平均为 0.69，具有明显的 Sr 负异常(图 9a, 表 3)。变质成因磷灰石表现出轻稀土元素亏损， $(La/Yb)_N$  比值为 0.13~2.03，平均为 0.68；具有 Eu 正异常与负异常( $\delta Eu = 0.25 \sim 1.08$ )，平均为 0.69。不同成因磷灰石的微量元素特征与 O'Sullivan et al. (2020) 报道的一致。②在中级变质阶段，斜长角闪岩样品 22WT-07 和 22WT-22 表现完全不同于岩浆成因的磷灰石微量元素特征，其微量元素含量低，稀土总量和轻稀土含量等都远低于绿片岩和基性麻粒岩样品，整体没有表现出从 LREE 至 HREE 的下降趋势，存在 Sr 正异常与负异常 2 种情况(图 9b)。其  $(La/Yb)_N$  比值为 0.06~1.05，平均为 0.44；具有 Eu 正异常与负异常( $\delta Eu = 0.12 \sim 1.12$ )，平均为 0.74。因此推断在这一变质阶段基本只有变质成因磷灰石存在。③在高级变质阶段，基性麻粒岩样品 22WT-09 和 22WT-12 具有轻稀土富集以及十分突出的 Sr 同位素负异常(图 9c)。因此推断在这一阶段基本只有岩浆成因磷灰石存在，其  $(La/Yb)_N$  比值为 2.54~34.19，平均为 14.04；具有 Eu 负异常( $\delta Eu = 0.39 \sim 0.97$ )，平均值为 0.67。

结合微量元素特征与成因类型区分，可对照上文中不同变质程度岩石中的磷灰石的形态学给予进一步匹配。例如，岩浆成因磷灰石颗粒在 CL 图中普遍呈自形至半自形，晶体形状较为完整，结构较为均一(Bruand et al., 2017; Sun et al., 2021)。变质成因磷灰石在 CL 图中普遍呈半自形至他形，有些磷灰石里有核，有不规则分区，结构不均一，边部或者整体存在裂隙(图 5)。

### 4.2 磷灰石微量元素组成对变质过程的约束

研究表明，全岩记录的地球化学信息只是样品的平均值，无法反映演化过程中的信息；磷灰石作为副矿物，能记录全岩地球化学无法记录的信息，如岩浆源区不均一、地壳混染作用和晚期变质、交代作用等(Chu et al., 2009; Nathwani et al., 2020)。

绿片岩样品 22WT-03 和 22WT-21 中的变质成因磷灰石明显亏损 LREE，但全岩却表现出 LREE 富集(图 7a)，这表明在变质作用过程中除了磷灰石，全岩 REE 配分还受到其他矿物的影响。这种差别可能是富 LREE 矿物结晶与磷灰石竞争导致的，可

表 3 五台—恒山地区变基性岩浆成因磷灰石微量元素组成 ( $\times 10^{-6}$ )

Table 3 Trace element compositions of magmatic apatite in metabasic rocks from the Wutai-Hengshan area ( $\times 10^{-6}$ )

| 样品号      | Rb   | Sr      | Y       | Zr     | Ba    | Ga   | La    | Ce     | Pr    | Nd     | Sm     | Eu    | Gd     | Tb    | Dy     | Ho    | Er     | Tm    | Yb     | Lu    | Hf    | Nb   | Ta | Pb    | Th    | U     | (La/Yb) <sub>N</sub> | $\delta$ Eu |
|----------|------|---------|---------|--------|-------|------|-------|--------|-------|--------|--------|-------|--------|-------|--------|-------|--------|-------|--------|-------|-------|------|----|-------|-------|-------|----------------------|-------------|
| Ap-03-2  | 0.03 | 1368.16 | 211.21  | 0.28   | 0.68  | 3.41 | 17.86 | 94.98  | 25.52 | 195.47 | 64.37  | 16.93 | 61.55  | 7.52  | 40.58  | 7.49  | 19.22  | 2.42  | 14.94  | 2.14  | 0     | 0    | 0  | 7.2   | 2.3   | 11.06 | 0.81                 | 0.82        |
| Ap-03-3  | 0.05 | 1004.23 | 296.07  | 0.1    | 0.42  | 2.44 | 10.16 | 65.76  | 19.06 | 162.25 | 61.25  | 17.09 | 69.89  | 9.26  | 55.28  | 11.22 | 28.42  | 3.69  | 22.18  | 3.08  | 0     | 0    | 0  | 8.62  | 2.35  | 8.91  | 0.31                 | 0.8         |
| Ap-03-5  | 0.32 | 1396.01 | 315.92  | 0.27   | 1.13  | 3.28 | 18.47 | 108.84 | 29.5  | 228.15 | 63.76  | 17.67 | 63.88  | 9.38  | 60.91  | 12.21 | 30.68  | 3.75  | 20.79  | 2.55  | 0     | 0.03 | 0  | 7.13  | 3.4   | 3.33  | 0.6                  | 0.84        |
| Ap-03-6  | 0.18 | 367.66  | 1340.29 | 0.04   | 0.21  | 7.86 | 90.85 | 361.61 | 71.45 | 430.42 | 181.11 | 17.02 | 244.68 | 43.53 | 262.76 | 48.27 | 125.31 | 16.59 | 106.09 | 13.88 | 0     | 0    | 0  | 6.58  | 4.02  | 5.11  | 0.58                 | 0.25        |
| Ap-03-10 | 0    | 400.93  | 277.6   | 0.12   | 0.38  | 5.04 | 61.86 | 223.69 | 41.29 | 243.34 | 66.91  | 15.85 | 80.09  | 9.31  | 49.3   | 9.67  | 25.2   | 3.19  | 18.84  | 3.07  | 0     | 0    | 0  | 4.01  | 4.4   | 3.18  | 2.23                 | 0.66        |
| Ap-03-11 | 0.06 | 3514.45 | 496.51  | 0      | 0     | 0.87 | 3.4   | 14.53  | 3.42  | 27.13  | 16.93  | 7.58  | 44.2   | 9.37  | 78.37  | 18.61 | 47.6   | 4.62  | 17.23  | 1.39  | 0     | 0    | 0  | 7.44  | 0.01  | 0     | 0                    | 0.84        |
| Ap-03-12 | 0.28 | 680.29  | 509.08  | 0.15   | 0.49  | 1.37 | 7.57  | 29.7   | 6.22  | 45.09  | 19.65  | 10.8  | 49.3   | 12.85 | 99.75  | 20.92 | 53.53  | 6.51  | 36.49  | 4.15  | 0     | 0    | 0  | 12.46 | 5.52  | 5.43  | 0.14                 | 1.06        |
| Ap-03-15 | 0.06 | 590.07  | 378.58  | 0.38   | 0.25  | 5.19 | 86.02 | 278.72 | 42.66 | 208.67 | 38.25  | 15.59 | 50.64  | 9.32  | 68.37  | 14    | 37.43  | 4.72  | 30.12  | 3.87  | 0     | 0    | 0  | 10.25 | 11.55 | 4.28  | 1.94                 | 1.08        |
| Ap-03-16 | 0.06 | 1536.28 | 400.4   | 0.44   | 0.93  | 5.73 | 36.02 | 195.81 | 53.63 | 424.94 | 134.48 | 31.84 | 133.31 | 15.13 | 77.7   | 14.2  | 35.62  | 4.49  | 26.12  | 3.88  | 0     | 0.01 | 0  | 9.36  | 1.11  | 12.28 | 0.94                 | 0.72        |
| Ap-03-20 | 0.14 | 713.26  | 704.28  | 1.81   | 0.88  | 3.05 | 25.82 | 99.77  | 20.58 | 140.25 | 63.02  | 17.53 | 104.35 | 20.36 | 142.86 | 27.93 | 70.25  | 8.6   | 48.61  | 5.58  | 0.02  | 0    | 0  | 13.05 | 5.44  | 8.91  | 0.36                 | 0.66        |
| Ap-21-2  | 0.19 | 2541.29 | 234.71  | 43.83  | 1.29  | 0.63 | 1.57  | 6.63   | 1.61  | 12.12  | 8.03   | 3.4   | 19.56  | 4.35  | 34.53  | 8.82  | 23.31  | 2.24  | 8.16   | 0.62  | 1.04  | -    | -  | 5.43  | 0.02  | -     | 0.13                 | 0.83        |
| Ap-21-3  | 0.12 | 3120.9  | 411.41  | 310.55 | 0.65  | 1.34 | 17.83 | 43.35  | 7.04  | 36.6   | 15.44  | 5.55  | 32.7   | 6.56  | 57.17  | 14.8  | 42.15  | 4.44  | 19.46  | 1.75  | 8.63  | -    | -  | 7.35  | 5.47  | -     | 0.62                 | 0.75        |
| Ap-21-4  | 0.03 | 3577.44 | 471.93  | 1.04   | 0     | 0.75 | 3.5   | 15.55  | 3.52  | 28.49  | 19.27  | 8.4   | 48.87  | 10.15 | 80.46  | 17.99 | 45.16  | 4.26  | 15.77  | 1.38  | 0.04  | -    | -  | 7.51  | 0.02  | -     | 0.15                 | 0.83        |
| Ap-21-5  | 1.4  | 3460.81 | 418.28  | 0.02   | 11.13 | 1.24 | 4.06  | 16.16  | 3.83  | 29.19  | 17.46  | 7.39  | 42.59  | 8.55  | 67.3   | 15.87 | 38.51  | 3.65  | 13.88  | 1.09  | 0     | -    | -  | 7.24  | 2.24  | -     | 0.2                  | 0.83        |
| Ap-21-6  | 2.12 | 1051.97 | 84.37   | 104.44 | 48.64 | 1.28 | 11.56 | 30.85  | 4.65  | 23.65  | 6.31   | 1.77  | 8.74   | 1.64  | 13.2   | 2.9   | 8.3    | 0.98  | 5.12   | 0.53  | 2.55  | -    | -  | 2.67  | 4.93  | -     | 1.53                 | 0.73        |
| Ap-21-7  | 0.06 | 3547.7  | 459.25  | 710.89 | 0     | 0.85 | 3.16  | 13.83  | 3.29  | 27.35  | 17.51  | 8.09  | 46.13  | 9.45  | 75.56  | 16.63 | 41.57  | 4.08  | 16.33  | 1.69  | 19.92 | -    | -  | 8.54  | 0.06  | -     | 0.13                 | 0.87        |
| Ap-21-8  | 0.08 | 3476.36 | 399.06  | 15.65  | 0     | 0.92 | 2.84  | 11.96  | 2.87  | 22.26  | 13.67  | 6.52  | 35.76  | 7.89  | 64.21  | 14.77 | 37.38  | 3.59  | 12.79  | 1.09  | 0.43  | -    | -  | 7.35  | 0.26  | -     | 0.15                 | 0.9         |
| Ap-21-9  | 0.09 | 2984.42 | 305.04  | 25.91  | 0.36  | 1.33 | 12.68 | 33.04  | 4.77  | 25.79  | 11.75  | 4.86  | 26.74  | 5.67  | 46.4   | 10.95 | 29.01  | 2.84  | 10.24  | 0.87  | 0.56  | -    | -  | 6.72  | 1.45  | -     | 0.84                 | 0.84        |
| Ap-21-11 | 0.05 | 3517.78 | 500.66  | -      | 0     | 0.91 | 3.55  | 14.91  | 3.51  | 27.66  | 18.25  | 7.84  | 47.01  | 10.19 | 83.51  | 18.66 | 46.43  | 4.21  | 15.35  | 1.28  | 0     | -    | -  | 7.5   | 0.01  | -     | 0.16                 | 0.82        |
| Ap-07-1  | 0.01 | 379.37  | 2.94    | 0      | 1.25  | 0.67 | 0.76  | 1.88   | 0.26  | 1.84   | 0.6    | 0.16  | 0.57   | 0.08  | 0.51   | 0.11  | 0.38   | 0.08  | 0.49   | 0.08  | 0     | 0    | 0  | 0.78  | 0.02  | 0.11  | 1.05                 | 0.85        |
| Ap-07-2  | -    | 360.8   | 4.31    | 0      | 0.71  | 0.84 | 0.47  | 1.16   | 0.17  | 0.93   | 0.39   | 0.09  | 0.82   | 0.09  | 0.49   | 0.16  | 0.58   | 0.1   | 0.69   | 0.14  | 0     | 0    | 0  | 0.64  | 0.01  | 0.07  | 0.46                 | 0.46        |
| Ap-07-3  | 0.18 | 312.5   | 4.89    | 0.01   | 0.46  | 0.75 | 0.78  | 1.3    | 0.23  | 1.6    | 0.38   | 0.1   | 0.78   | 0.12  | 0.66   | 0.17  | 0.63   | 0.11  | 0.9    | 0.18  | 0     | 0    | 0  | 0.52  | 0.02  | 0.05  | 0.59                 | 0.54        |
| Ap-07-4  | -    | 312.78  | 3.28    | 0      | 0.42  | 0.87 | 0.18  | 0.44   | 0.05  | 0.4    | 0.17   | 0.01  | 0.31   | 0.05  | 0.37   | 0.12  | 0.4    | 0.1   | 0.7    | 0.08  | 0     | 0    | 0  | 0.51  | 0.04  | 0.06  | 0.18                 | 0.12        |
| Ap-07-5  | 0.44 | 370.84  | 3.57    | 0.09   | 4.94  | 1.24 | 0.88  | 2.19   | 0.3   | 2.09   | 0.38   | 0.11  | 0.74   | 0.09  | 0.45   | 0.14  | 0.51   | 0.07  | 0.69   | 0.13  | 0     | 0    | 0  | 0.73  | 0.01  | 0.08  | 0.87                 | 0.61        |
| Ap-07-6  | 0    | 328.42  | 2.55    | 0.19   | 0.51  | 0.72 | 0.1   | 0.2    | 0.03  | 0.23   | 0.08   | 0.01  | 0.09   | 0.03  | 0.28   | 0.08  | 0.31   | 0.07  | 0.51   | 0.11  | 0     | 0    | 0  | 0.56  | 0.03  | 0.09  | 0.13                 | 0.33        |
| Ap-07-7  | 0    | 440.71  | 3.92    | 1.51   | 1.24  | 0.96 | 0.94  | 2.28   | 0.36  | 2.26   | 0.54   | 0.2   | 1.16   | 0.12  | 0.75   | 0.16  | 0.47   | 0.07  | 0.63   | 0.1   | 0.05  | 0    | 0  | 1.01  | 0.01  | 0.07  | 1.01                 | 0.79        |
| Ap-07-8  | 0.01 | 335.44  | 2.18    | 0      | 0.37  | 0.82 | 0.14  | 0.2    | 0.03  | 0.27   | 0.05   | 0.01  | 0.15   | 0.03  | 0.21   | 0.08  | 0.36   | 0.05  | 0.5    | 0.12  | 0     | 0    | 0  | 0.52  | 0     | 0.07  | 0.18                 | 0.53        |

续表 3

| 样品点号     | Rb   | Sr     | Y      | Zr    | Ba   | Ga   | La   | Ce    | Pr   | Nd    | Sm    | Eu   | Gd    | Tb   | Dy    | Ho   | Er    | Tm   | Yb    | Lu   | Hf   | Nb   | Ta | Pb   | Th   | U    | (La/Yb) <sub>N</sub> | $\delta\text{Eu}$ |
|----------|------|--------|--------|-------|------|------|------|-------|------|-------|-------|------|-------|------|-------|------|-------|------|-------|------|------|------|----|------|------|------|----------------------|-------------------|
| Ap-07-9  | 0.01 | 243.68 | 5.52   | 0     | 0.29 | 0.68 | 0.08 | 0.14  | 0.02 | 0.14  | 0.03  | 0.01 | 0.17  | 0.05 | 0.55  | 0.18 | 0.74  | 0.1  | 0.91  | 0.18 | 0    | 0    | 0  | 0.38 | 0    | 0.12 | 0.06                 | 0.64              |
| Ap-07-10 | 0    | 303.45 | 24.04  | 0.44  | 0.54 | 0.83 | 1.56 | 4.63  | 0.84 | 4.86  | 1.79  | 0.67 | 3.25  | 0.53 | 4.13  | 0.94 | 3.29  | 0.54 | 4.87  | 0.93 | 0    | 0.01 | 0  | 1.19 | 5.22 | 0.08 | 0.22                 | 0.85              |
| Ap-07-11 | 0.03 | 342.21 | 105.74 | 2.13  | 0.59 | 1.02 | 7.83 | 23.13 | 4.04 | 23.98 | 9.55  | 3.45 | 16.7  | 2.82 | 18.24 | 4.31 | 12.4  | 1.73 | 13.57 | 2.53 | 0    | 0    | 0  | 1.11 | 2.97 | 0.02 | 0.39                 | 0.83              |
| Ap-07-12 | 0    | 221.87 | 4.24   | 0     | 0.42 | 0.74 | 0.09 | 0.24  | 0.03 | 0.33  | 0.13  | 0.02 | 0.3   | 0.07 | 0.47  | 0.16 | 0.56  | 0.12 | 0.8   | 0.15 | 0    | 0    | 0  | 0.42 | 0    | 0.03 | 0.08                 | 0.36              |
| Ap-07-13 | -    | 369.02 | 35.61  | 84.63 | 0.45 | 0.96 | 2.18 | 6.89  | 1.27 | 7.67  | 3.16  | 1.02 | 5.16  | 0.94 | 5.85  | 1.45 | 4.15  | 0.62 | 4.66  | 0.82 | 1.98 | 0    | 0  | 1.23 | 2.21 | 0.65 | 0.32                 | 0.77              |
| Ap-07-14 | -    | 313.06 | 4.55   | 0.01  | 0.87 | 0.7  | 0.1  | 0.21  | 0.03 | 0.27  | 0.1   | 0.03 | 0.37  | 0.07 | 0.55  | 0.16 | 0.68  | 0.12 | 0.94  | 0.18 | 0    | 0    | 0  | 0.51 | 0.39 | 0.07 | 0.07                 | 0.47              |
| Ap-22-1  | 0    | 184.15 | 99.84  | 0     | 0.17 | 0.9  | 3.97 | 15.11 | 3.62 | 27.59 | 14.61 | 5.84 | 21.41 | 3.22 | 19.21 | 3.58 | 9.16  | 1.08 | 5.61  | 0.67 | 0    | -    | -  | 0.57 | 0    | -    | 0.48                 | 1.01              |
| Ap-22-2  | 0    | 185.64 | 152.79 | 0     | 0.18 | 0.76 | 3.62 | 13.6  | 3.4  | 26.77 | 17.04 | 6.33 | 29.14 | 4.89 | 29.73 | 5.83 | 14.31 | 1.62 | 8.3   | 1    | 0    | -    | -  | 0.56 | 0.01 | -    | 0.3                  | 0.87              |
| Ap-22-3  | 0.01 | 177.59 | 64.89  | 0     | 0.29 | 0.9  | 3.48 | 14.66 | 3.58 | 25.88 | 12.64 | 5.11 | 16.03 | 2.2  | 11.92 | 2.3  | 5.97  | 0.64 | 3.83  | 0.59 | 0    | -    | -  | 0.92 | 0    | -    | 0.62                 | 1.1               |
| Ap-22-4  | 0.14 | 211.54 | 81.79  | 0.04  | 0.22 | 1.04 | 3.55 | 16.16 | 4.08 | 30.14 | 15.09 | 4.91 | 20.47 | 3.05 | 16.92 | 3.04 | 7.78  | 0.92 | 4.82  | 0.68 | 0    | -    | -  | 1.5  | 0.01 | -    | 0.5                  | 0.85              |
| Ap-22-5  | 0.03 | 183.41 | 149.24 | 0     | 0    | 1.11 | 3.41 | 14.81 | 3.68 | 31.45 | 19.64 | 5.74 | 30.47 | 5.06 | 27.99 | 5.23 | 11.89 | 1.29 | 6.47  | 0.82 | 0    | -    | -  | 0.47 | 0    | -    | 0.36                 | 0.72              |
| Ap-22-6  | 0.04 | 161.4  | 46.19  | 0     | 0.37 | 0.88 | 2.12 | 11.38 | 3.25 | 25.04 | 11.11 | 4.2  | 11.72 | 1.72 | 9.14  | 1.67 | 4.23  | 0.53 | 3.11  | 0.41 | 0    | -    | -  | 0.79 | 0.01 | -    | 0.46                 | 1.12              |
| Ap-22-7  | 0.03 | 189.95 | 80.26  | -     | 0.17 | 0.89 | 3.68 | 14.65 | 3.63 | 27.58 | 15.01 | 4.56 | 20.06 | 2.76 | 16.16 | 2.82 | 7.24  | 0.77 | 4.12  | 0.5  | 0    | -    | -  | 1.02 | 0    | -    | 0.61                 | 0.8               |
| Ap-22-8  | 0    | 191.69 | 100.46 | 0     | 0    | 0.84 | 3.23 | 13.76 | 3.51 | 28.49 | 15.54 | 5.45 | 22.08 | 3.34 | 19.13 | 3.69 | 9.29  | 1.11 | 5.68  | 0.75 | 0    | -    | -  | 0.42 | 0.01 | -    | 0.39                 | 0.9               |
| Ap-22-9  | 0    | 186.33 | 121.87 | 0     | 0.16 | 0.8  | 3.9  | 15.23 | 3.57 | 26.74 | 14.89 | 6.22 | 23.94 | 3.81 | 23.66 | 4.55 | 11.84 | 1.39 | 8.11  | 0.95 | 0    | -    | -  | 0.95 | 0.01 | -    | 0.33                 | 1                 |
| Ap-22-10 | 0.25 | 193.79 | 169    | 45.78 | 0.55 | 1.25 | 4.95 | 19.56 | 4.5  | 33.69 | 19    | 5.87 | 31.62 | 4.97 | 30.63 | 6.13 | 15.53 | 1.76 | 9.8   | 1.19 | 1.27 | -    | -  | 0.56 | 0.02 | -    | 0.34                 | 0.73              |
| Ap-22-11 | 0.08 | 184.26 | 148.02 | 0     | 0.25 | 0.96 | 4.24 | 16.11 | 3.96 | 29.57 | 16.53 | 5.73 | 27.79 | 4.56 | 28.27 | 5.77 | 14.57 | 1.64 | 8.95  | 1.04 | 0    | -    | -  | 0.42 | 0.01 | -    | 0.32                 | 0.81              |
| Ap-22-12 | -    | 177.85 | 55.42  | 1.39  | 0.2  | 0.78 | 3.95 | 14.74 | 3.31 | 24.43 | 11.95 | 4.48 | 15.02 | 2.09 | 11.53 | 2.05 | 5.1   | 0.61 | 3.67  | 0.46 | 0.02 | -    | -  | 0.94 | 0    | -    | 0.73                 | 1.02              |
| Ap-22-13 | 0.01 | 178.61 | 101.4  | 0     | 0.2  | 1.1  | 3.12 | 13.43 | 3.29 | 26.7  | 14.79 | 5.57 | 21.88 | 3.25 | 20.13 | 3.81 | 10.13 | 1.1  | 6.35  | 0.82 | 0    | -    | -  | 0.85 | 0    | -    | 0.33                 | 0.94              |
| Ap-22-14 | 0    | 197.55 | 62.3   | 0     | 0.11 | 0.8  | 2.27 | 11.49 | 2.93 | 23.35 | 10.66 | 3.25 | 13.73 | 2.06 | 12.26 | 2.45 | 6.39  | 0.78 | 4.16  | 0.49 | 0    | -    | -  | 1.33 | 0.01 | -    | 0.37                 | 0.82              |
| Ap-22-15 | 0.12 | 172.03 | 61.61  | 0     | 0.22 | 0.93 | 3.46 | 16.78 | 4.04 | 29.51 | 11.54 | 2.99 | 12.34 | 1.88 | 11.1  | 2.28 | 6.08  | 0.79 | 4.88  | 0.8  | 0    | -    | -  | 0.94 | 0    | -    | 0.48                 | 0.76              |
| Ap-22-16 | 0    | 179.23 | 104.41 | 0     | 0.25 | 0.62 | 3.53 | 14.85 | 3.51 | 29.62 | 17    | 5.36 | 26.23 | 3.71 | 20.08 | 4    | 9.64  | 1.06 | 5.6   | 0.62 | 0    | -    | -  | 0.32 | 0    | -    | 0.43                 | 0.77              |
| Ap-22-17 | 0    | 192.03 | 110.25 | 0     | 0.11 | 0.84 | 4.34 | 17.93 | 4.12 | 33.57 | 19.55 | 5.36 | 29.49 | 4.15 | 23.07 | 4.32 | 10.41 | 1.2  | 5.61  | 0.67 | 0    | -    | -  | 0.3  | 0    | -    | 0.53                 | 0.68              |
| Ap-22-18 | -    | 189.31 | 111.03 | 0     | 0    | 0.77 | 3.73 | 16.01 | 3.72 | 29.33 | 18.51 | 5.44 | 28.42 | 4.04 | 23.24 | 4.26 | 9.64  | 0.99 | 4.83  | 0.61 | 0    | -    | -  | 0.41 | 0    | -    | 0.52                 | 0.72              |

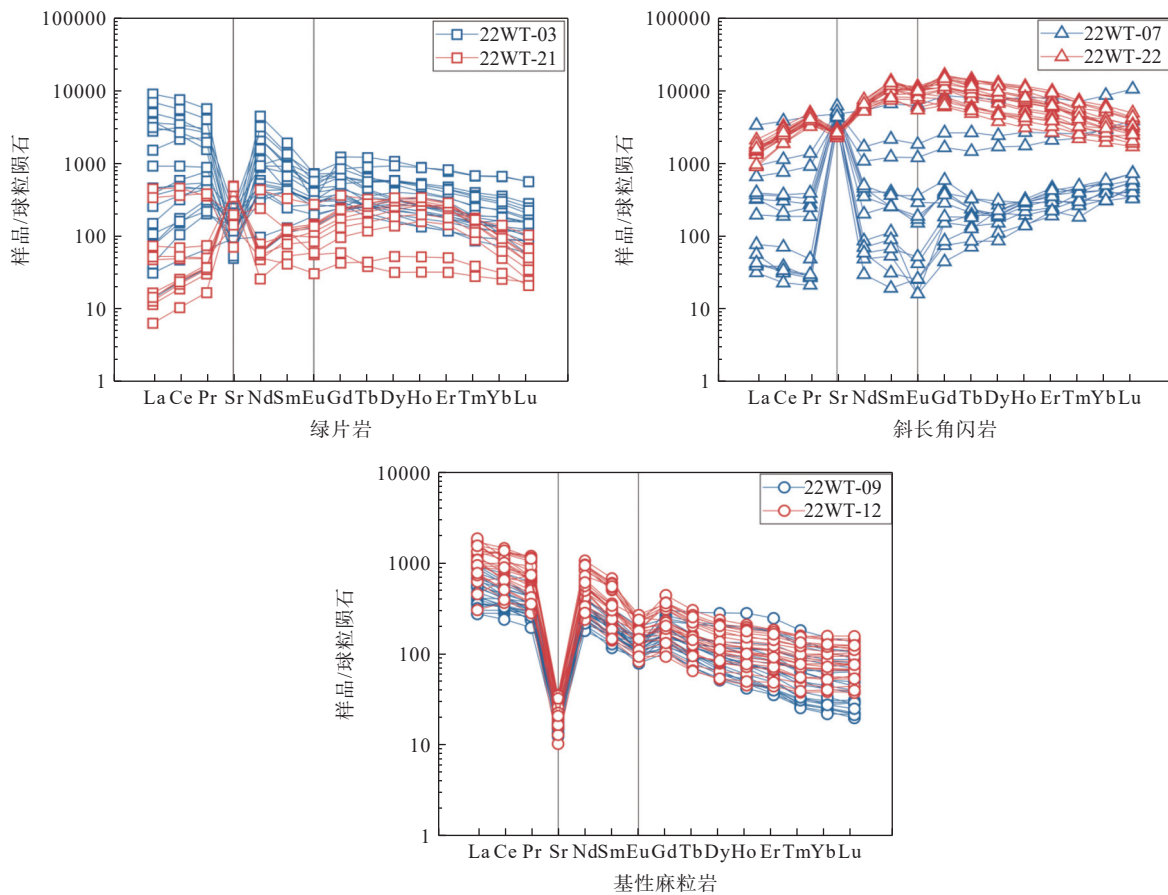
表 4 五台—恒山地区变基性岩变质成因磷灰石微量元素组成 ( $\times 10^{-6}$ )

Table 4 Trace element compositions of metamorphic apatite in metabasic rocks from the Wutai-Hengshan area ( $\times 10^{-6}$ )

| 样品号      | Rb   | Sr      | Y       | Zr     | Ba    | Ga   | La    | Ce     | Pr    | Nd     | Sm     | Eu    | Gd     | Tb    | Dy     | Ho    | Er     | Tm    | Yb     | Lu    | Hf    | Nb    | Ta | Pb    | Th    | U (La/Yb) <sub>0</sub> | Eu   |      |
|----------|------|---------|---------|--------|-------|------|-------|--------|-------|--------|--------|-------|--------|-------|--------|-------|--------|-------|--------|-------|-------|-------|----|-------|-------|------------------------|------|------|
| Ap-03-2  | 0.03 | 1368.16 | 211.21  | 0.28   | 0.68  | 3.41 | 17.86 | 94.98  | 25.52 | 195.47 | 64.37  | 16.93 | 61.55  | 7.52  | 40.58  | 7.49  | 19.22  | 2.42  | 14.94  | 2.14  | 0     | 0     | 0  | 7.2   | 2.3   | 11.06                  | 0.81 | 0.82 |
| Ap-03-3  | 0.05 | 1004.23 | 296.07  | 0.1    | 0.42  | 2.44 | 10.16 | 65.76  | 19.06 | 162.25 | 61.25  | 17.09 | 69.89  | 9.26  | 55.28  | 11.22 | 28.42  | 3.69  | 22.18  | 3.08  | 0     | 0     | 0  | 8.62  | 2.35  | 8.91                   | 0.31 | 0.8  |
| Ap-03-5  | 0.32 | 1396.01 | 315.92  | 0.27   | 1.13  | 3.28 | 18.47 | 108.84 | 29.5  | 228.15 | 63.76  | 17.67 | 63.88  | 9.38  | 60.91  | 12.21 | 30.68  | 3.75  | 20.79  | 2.55  | 0     | 0.003 | 0  | 7.13  | 3.4   | 3.33                   | 0.6  | 0.84 |
| Ap-03-6  | 0.18 | 367.66  | 1340.29 | 0.04   | 0.21  | 7.86 | 90.85 | 361.61 | 71.45 | 430.42 | 181.11 | 17.02 | 244.68 | 43.53 | 262.76 | 48.27 | 125.31 | 16.59 | 106.09 | 13.88 | 0     | 0     | 0  | 6.58  | 4.02  | 5.11                   | 0.58 | 0.25 |
| Ap-03-10 | 0    | 400.93  | 277.6   | 0.12   | 0.38  | 5.04 | 61.86 | 223.69 | 41.29 | 243.34 | 66.91  | 15.85 | 80.09  | 9.31  | 49.3   | 9.67  | 25.2   | 3.19  | 18.84  | 3.07  | 0     | 0     | 0  | 4.01  | 4.4   | 3.18                   | 2.23 | 0.66 |
| Ap-03-11 | 0.06 | 3514.45 | 496.51  | 0      | 0     | 0.87 | 3.4   | 14.53  | 3.42  | 27.13  | 16.93  | 7.58  | 44.2   | 9.37  | 78.37  | 18.61 | 47.6   | 4.62  | 17.23  | 1.39  | 0     | 0     | 0  | 7.44  | 0.01  | 0                      | 0    | 0.84 |
| Ap-03-12 | 0.28 | 680.29  | 509.08  | 0.15   | 0.49  | 1.37 | 7.57  | 29.7   | 6.22  | 45.09  | 19.65  | 10.8  | 49.3   | 12.85 | 99.75  | 20.92 | 53.53  | 6.51  | 36.49  | 4.15  | 0     | 0     | 0  | 12.46 | 5.52  | 5.43                   | 0.14 | 1.06 |
| Ap-03-15 | 0.06 | 590.07  | 378.58  | 0.38   | 0.25  | 5.19 | 86.02 | 278.72 | 42.66 | 208.67 | 38.25  | 15.59 | 50.64  | 9.32  | 68.37  | 14    | 37.43  | 4.72  | 30.12  | 3.87  | 0     | 0     | 0  | 10.25 | 11.55 | 4.28                   | 1.94 | 1.08 |
| Ap-03-16 | 0.06 | 1536.28 | 400.4   | 0.44   | 0.93  | 5.73 | 36.02 | 195.81 | 53.63 | 424.94 | 134.48 | 31.84 | 133.31 | 15.13 | 77.7   | 14.2  | 35.62  | 4.49  | 26.12  | 3.88  | 0     | 0.001 | 0  | 9.36  | 1.11  | 12.28                  | 0.94 | 0.72 |
| Ap-03-20 | 0.14 | 713.26  | 704.28  | 1.81   | 0.88  | 3.05 | 25.82 | 99.77  | 20.58 | 140.25 | 63.02  | 17.53 | 104.35 | 20.36 | 142.86 | 27.93 | 70.25  | 8.6   | 48.61  | 5.58  | 0.02  | 0     | 0  | 13.05 | 5.44  | 8.91                   | 0.36 | 0.66 |
| Ap-21-2  | 0.19 | 2541.29 | 234.71  | 43.83  | 1.29  | 0.63 | 1.57  | 6.63   | 1.61  | 12.12  | 8.03   | 3.4   | 19.56  | 4.35  | 34.53  | 8.82  | 23.31  | 2.24  | 8.16   | 0.62  | 1.04  | -     | -  | 5.43  | 0.02  | -                      | 0.13 | 0.83 |
| Ap-21-3  | 0.12 | 3120.9  | 411.41  | 310.55 | 0.65  | 1.34 | 17.83 | 43.35  | 7.04  | 36.6   | 15.44  | 5.55  | 32.7   | 6.56  | 57.17  | 14.8  | 42.15  | 4.44  | 19.46  | 1.75  | 8.63  | -     | -  | 7.35  | 5.47  | -                      | 0.62 | 0.75 |
| Ap-21-4  | 0.03 | 3577.44 | 471.93  | 1.04   | 0     | 0.75 | 3.5   | 15.55  | 3.52  | 28.49  | 19.27  | 8.4   | 48.87  | 10.15 | 80.46  | 17.99 | 45.16  | 4.26  | 15.77  | 1.38  | 0.04  | -     | -  | 7.51  | 0.02  | -                      | 0.15 | 0.83 |
| Ap-21-5  | 1.4  | 3460.81 | 418.28  | 0.02   | 11.13 | 1.24 | 4.06  | 16.16  | 3.83  | 29.19  | 17.46  | 7.39  | 42.59  | 8.55  | 67.3   | 15.87 | 38.51  | 3.65  | 13.88  | 1.09  | 0     | -     | -  | 7.24  | 2.24  | -                      | 0.2  | 0.83 |
| Ap-21-6  | 2.12 | 1051.97 | 84.37   | 104.44 | 48.64 | 1.28 | 11.56 | 30.85  | 4.65  | 23.65  | 6.31   | 1.77  | 8.74   | 1.64  | 13.2   | 2.9   | 8.3    | 0.98  | 5.12   | 0.53  | 2.55  | -     | -  | 2.67  | 4.93  | -                      | 1.53 | 0.73 |
| Ap-21-7  | 0.06 | 3547.7  | 459.25  | 710.89 | 0     | 0.85 | 3.16  | 13.83  | 3.29  | 27.35  | 17.51  | 8.09  | 46.13  | 9.45  | 75.56  | 16.63 | 41.57  | 4.08  | 16.33  | 1.69  | 19.92 | -     | -  | 8.54  | 0.06  | -                      | 0.13 | 0.87 |
| Ap-21-8  | 0.08 | 3476.36 | 399.06  | 15.65  | 0     | 0.92 | 2.84  | 11.96  | 2.87  | 22.26  | 13.67  | 6.52  | 35.76  | 7.89  | 64.21  | 14.77 | 37.38  | 3.59  | 12.79  | 1.09  | 0.43  | -     | -  | 7.35  | 0.26  | -                      | 0.15 | 0.9  |
| Ap-21-9  | 0.09 | 2984.42 | 305.04  | 25.91  | 0.36  | 1.33 | 12.68 | 33.04  | 4.77  | 25.79  | 11.75  | 4.86  | 26.74  | 5.67  | 46.4   | 10.95 | 29.01  | 2.84  | 10.24  | 0.87  | 0.56  | -     | -  | 6.72  | 1.45  | -                      | 0.84 | 0.84 |
| Ap-21-11 | 0.05 | 3517.78 | 500.66  | -      | 0     | 0.91 | 3.55  | 14.91  | 3.51  | 27.66  | 18.25  | 7.84  | 47.01  | 10.19 | 83.51  | 18.66 | 46.43  | 4.21  | 15.35  | 1.28  | 0     | -     | -  | 7.5   | 0.01  | -                      | 0.16 | 0.82 |
| Ap-07-1  | 0.01 | 379.37  | 2.94    | 0      | 1.25  | 0.67 | 0.76  | 1.88   | 0.26  | 1.84   | 0.6    | 0.16  | 0.57   | 0.08  | 0.51   | 0.11  | 0.38   | 0.08  | 0.49   | 0.08  | 0     | 0     | 0  | 0.78  | 0.02  | 0.11                   | 1.05 | 0.85 |
| Ap-07-2  | -    | 360.8   | 4.31    | 0      | 0.71  | 0.84 | 0.47  | 1.16   | 0.17  | 0.93   | 0.39   | 0.09  | 0.82   | 0.09  | 0.49   | 0.16  | 0.58   | 0.1   | 0.69   | 0.14  | 0     | 0     | 0  | 0.64  | 0.01  | 0.07                   | 0.46 | 0.46 |
| Ap-07-3  | 0.18 | 312.5   | 4.89    | 0.01   | 0.46  | 0.75 | 0.78  | 1.3    | 0.23  | 1.6    | 0.38   | 0.1   | 0.78   | 0.12  | 0.66   | 0.17  | 0.63   | 0.11  | 0.9    | 0.18  | 0     | 0     | 0  | 0.52  | 0.02  | 0.05                   | 0.59 | 0.54 |
| Ap-07-4  | -    | 312.78  | 3.28    | 0      | 0.42  | 0.87 | 0.18  | 0.44   | 0.05  | 0.4    | 0.17   | 0.01  | 0.31   | 0.05  | 0.37   | 0.12  | 0.4    | 0.1   | 0.7    | 0.08  | 0     | 0     | 0  | 0.51  | 0.04  | 0.06                   | 0.18 | 0.12 |
| Ap-07-5  | 0.44 | 370.84  | 3.57    | 0.09   | 4.94  | 1.24 | 0.88  | 2.19   | 0.3   | 2.09   | 0.38   | 0.11  | 0.74   | 0.09  | 0.45   | 0.14  | 0.51   | 0.07  | 0.69   | 0.13  | 0     | 0     | 0  | 0.73  | 0.01  | 0.08                   | 0.87 | 0.61 |
| Ap-07-6  | 0    | 328.42  | 2.55    | 0.19   | 0.51  | 0.72 | 0.1   | 0.2    | 0.03  | 0.23   | 0.08   | 0.01  | 0.09   | 0.03  | 0.28   | 0.08  | 0.31   | 0.07  | 0.51   | 0.11  | 0     | 0     | 0  | 0.56  | 0.03  | 0.09                   | 0.13 | 0.33 |
| Ap-07-7  | 0    | 440.71  | 3.92    | 1.51   | 1.24  | 0.96 | 0.94  | 2.28   | 0.36  | 2.26   | 0.54   | 0.2   | 1.16   | 0.12  | 0.75   | 0.16  | 0.47   | 0.07  | 0.63   | 0.1   | 0.05  | 0     | 0  | 1.01  | 0.01  | 0.07                   | 1.01 | 0.79 |

续表 4

| 样品点号     | Rb   | Sr     | Y      | Zr    | Ba   | Ga   | La   | Ce    | Pr   | Nd    | Sm    | Eu   | Gd    | Tb   | Dy    | Ho   | Er    | Tm   | Yb    | Lu   | Hf   | Nb   | Ta | Pb   | Th   | U    | (La/Yb) <sub>n</sub> dEu |      |
|----------|------|--------|--------|-------|------|------|------|-------|------|-------|-------|------|-------|------|-------|------|-------|------|-------|------|------|------|----|------|------|------|--------------------------|------|
| Ap-07-8  | 0.01 | 335.44 | 2.18   | 0     | 0.37 | 0.82 | 0.14 | 0.2   | 0.03 | 0.27  | 0.05  | 0.01 | 0.15  | 0.03 | 0.21  | 0.08 | 0.36  | 0.05 | 0.5   | 0.12 | 0    | 0    | 0  | 0.52 | 0    | 0.07 | 0.18                     | 0.53 |
| Ap-07-9  | 0.01 | 243.68 | 5.52   | 0     | 0.29 | 0.68 | 0.08 | 0.14  | 0.02 | 0.14  | 0.03  | 0.01 | 0.17  | 0.05 | 0.55  | 0.18 | 0.74  | 0.1  | 0.91  | 0.18 | 0    | 0    | 0  | 0.38 | 0    | 0.12 | 0.06                     | 0.64 |
| Ap-07-10 | 0    | 303.45 | 24.04  | 0.44  | 0.54 | 0.83 | 1.56 | 4.63  | 0.84 | 4.86  | 1.79  | 0.67 | 3.25  | 0.53 | 4.13  | 0.94 | 3.29  | 0.54 | 4.87  | 0.93 | 0    | 0.01 | 0  | 1.19 | 5.22 | 0.08 | 0.22                     | 0.85 |
| Ap-07-11 | 0.03 | 342.21 | 105.74 | 2.13  | 0.59 | 1.02 | 7.83 | 23.13 | 4.04 | 23.98 | 9.55  | 3.45 | 16.7  | 2.82 | 18.24 | 4.31 | 12.4  | 1.73 | 13.57 | 2.53 | 0    | 0    | 0  | 1.11 | 2.97 | 0.02 | 0.39                     | 0.83 |
| Ap-07-12 | 0    | 221.87 | 4.24   | 0     | 0.42 | 0.74 | 0.09 | 0.24  | 0.03 | 0.33  | 0.13  | 0.02 | 0.3   | 0.07 | 0.47  | 0.16 | 0.56  | 0.12 | 0.8   | 0.15 | 0    | 0    | 0  | 0.42 | 0    | 0.03 | 0.08                     | 0.36 |
| Ap-07-13 | -    | 369.02 | 35.61  | 84.63 | 0.45 | 0.96 | 2.18 | 6.89  | 1.27 | 7.67  | 3.16  | 1.02 | 5.16  | 0.94 | 5.85  | 1.45 | 4.15  | 0.62 | 4.66  | 0.82 | 1.98 | 0    | 0  | 1.23 | 2.21 | 0.65 | 0.32                     | 0.77 |
| Ap-07-14 | -    | 313.06 | 4.55   | 0.01  | 0.87 | 0.7  | 0.1  | 0.21  | 0.03 | 0.27  | 0.1   | 0.03 | 0.37  | 0.07 | 0.55  | 0.16 | 0.68  | 0.12 | 0.94  | 0.18 | 0    | 0    | 0  | 0.51 | 0.39 | 0.07 | 0.07                     | 0.47 |
| Ap-22-1  | 0    | 184.15 | 99.84  | 0     | 0.17 | 0.9  | 3.97 | 15.11 | 3.62 | 27.59 | 14.61 | 5.84 | 21.41 | 3.22 | 19.21 | 3.58 | 9.16  | 1.08 | 5.61  | 0.67 | 0    | -    | -  | 0.57 | 0    | -    | 0.48                     | 1.01 |
| Ap-22-2  | 0    | 185.64 | 152.79 | 0     | 0.18 | 0.76 | 3.62 | 13.6  | 3.4  | 26.77 | 17.04 | 6.33 | 29.14 | 4.89 | 29.73 | 5.83 | 14.31 | 1.62 | 8.3   | 1    | 0    | -    | -  | 0.56 | 0.01 | -    | 0.3                      | 0.87 |
| Ap-22-3  | 0.01 | 177.59 | 64.89  | 0     | 0.29 | 0.9  | 3.48 | 14.66 | 3.58 | 25.88 | 12.64 | 5.11 | 16.03 | 2.2  | 11.92 | 2.3  | 5.97  | 0.64 | 3.83  | 0.59 | 0    | -    | -  | 0.92 | 0    | -    | 0.62                     | 1.1  |
| Ap-22-4  | 0.14 | 211.54 | 81.79  | 0.04  | 0.22 | 1.04 | 3.55 | 16.16 | 4.08 | 30.14 | 15.09 | 4.91 | 20.47 | 3.05 | 16.92 | 3.04 | 7.78  | 0.92 | 4.82  | 0.68 | 0    | -    | -  | 1.5  | 0.01 | -    | 0.5                      | 0.85 |
| Ap-22-5  | 0.03 | 183.41 | 149.24 | 0     | 0    | 1.11 | 3.41 | 14.81 | 3.68 | 31.45 | 19.64 | 5.74 | 30.47 | 5.06 | 27.99 | 5.23 | 11.89 | 1.29 | 6.47  | 0.82 | 0    | -    | -  | 0.47 | 0    | -    | 0.36                     | 0.72 |
| Ap-22-6  | 0.04 | 161.4  | 46.19  | 0     | 0.37 | 0.88 | 2.12 | 11.38 | 3.25 | 25.04 | 11.11 | 4.2  | 11.72 | 1.72 | 9.14  | 1.67 | 4.23  | 0.53 | 3.11  | 0.41 | 0    | -    | -  | 0.79 | 0.01 | -    | 0.46                     | 1.12 |
| Ap-22-7  | 0.03 | 189.95 | 80.26  | -     | 0.17 | 0.89 | 3.68 | 14.65 | 3.63 | 27.58 | 15.01 | 4.56 | 20.06 | 2.76 | 16.16 | 2.82 | 7.24  | 0.77 | 4.12  | 0.5  | 0    | -    | -  | 1.02 | 0    | -    | 0.61                     | 0.8  |
| Ap-22-8  | 0    | 191.69 | 100.46 | 0     | 0    | 0.84 | 3.23 | 13.76 | 3.51 | 28.49 | 15.54 | 5.45 | 22.08 | 3.34 | 19.13 | 3.69 | 9.29  | 1.11 | 5.68  | 0.75 | 0    | -    | -  | 0.42 | 0.01 | -    | 0.39                     | 0.9  |
| Ap-22-9  | 0    | 186.33 | 121.87 | 0     | 0.16 | 0.8  | 3.9  | 15.23 | 3.57 | 26.74 | 14.89 | 6.22 | 23.94 | 3.81 | 23.66 | 4.55 | 11.84 | 1.39 | 8.11  | 0.95 | 0    | -    | -  | 0.95 | 0.01 | -    | 0.33                     | 1    |
| Ap-22-10 | 0.25 | 193.79 | 169    | 45.78 | 0.55 | 1.25 | 4.95 | 19.56 | 4.5  | 33.69 | 19    | 5.87 | 31.62 | 4.97 | 30.63 | 6.13 | 15.53 | 1.76 | 9.8   | 1.19 | 1.27 | -    | -  | 0.56 | 0.02 | -    | 0.34                     | 0.73 |
| Ap-22-11 | 0.08 | 184.26 | 148.02 | 0     | 0.25 | 0.96 | 4.24 | 16.11 | 3.96 | 29.57 | 16.53 | 5.73 | 27.79 | 4.56 | 28.27 | 5.77 | 14.57 | 1.64 | 8.95  | 1.04 | 0    | -    | -  | 0.42 | 0.01 | -    | 0.32                     | 0.81 |
| Ap-22-12 | -    | 177.85 | 55.42  | 1.39  | 0.2  | 0.78 | 3.95 | 14.74 | 3.31 | 24.43 | 11.95 | 4.48 | 15.02 | 2.09 | 11.53 | 2.05 | 5.1   | 0.61 | 3.67  | 0.46 | 0.02 | -    | -  | 0.94 | 0    | -    | 0.73                     | 1.02 |
| Ap-22-13 | 0.01 | 178.61 | 101.4  | 0     | 0.2  | 1.1  | 3.12 | 13.43 | 3.29 | 26.7  | 14.79 | 5.57 | 21.88 | 3.25 | 20.13 | 3.81 | 10.13 | 1.1  | 6.35  | 0.82 | 0    | -    | -  | 0.85 | 0    | -    | 0.33                     | 0.94 |
| Ap-22-14 | 0    | 197.55 | 62.3   | 0     | 0.11 | 0.8  | 2.27 | 11.49 | 2.93 | 23.35 | 10.66 | 3.25 | 13.73 | 2.06 | 12.26 | 2.45 | 6.39  | 0.78 | 4.16  | 0.49 | 0    | -    | -  | 1.33 | 0.01 | -    | 0.37                     | 0.82 |
| Ap-22-15 | 0.12 | 172.03 | 61.61  | 0     | 0.22 | 0.93 | 3.46 | 16.78 | 4.04 | 29.51 | 11.54 | 2.99 | 12.34 | 1.88 | 11.1  | 2.28 | 6.08  | 0.79 | 4.88  | 0.8  | 0    | -    | -  | 0.94 | 0    | -    | 0.48                     | 0.76 |
| Ap-22-16 | 0    | 179.23 | 104.41 | 0     | 0.25 | 0.62 | 3.53 | 14.85 | 3.51 | 29.62 | 17    | 5.36 | 26.23 | 3.71 | 20.08 | 4    | 9.64  | 1.06 | 5.6   | 0.62 | 0    | -    | -  | 0.32 | 0    | -    | 0.43                     | 0.77 |
| Ap-22-17 | 0    | 192.03 | 110.25 | 0     | 0.11 | 0.84 | 4.34 | 17.93 | 4.12 | 33.57 | 19.55 | 5.36 | 29.49 | 4.15 | 23.07 | 4.32 | 10.41 | 1.2  | 5.61  | 0.67 | 0    | -    | -  | 0.3  | 0    | -    | 0.53                     | 0.68 |
| Ap-22-18 | -    | 189.31 | 111.03 | 0     | 0    | 0.77 | 3.73 | 16.01 | 3.72 | 29.33 | 18.51 | 5.44 | 28.42 | 4.04 | 23.24 | 4.26 | 9.64  | 0.99 | 4.83  | 0.61 | 0    | -    | -  | 0.41 | 0    | -    | 0.52                     | 0.72 |



a—绿片岩样品微量元素图解; b—斜长角闪岩样品微量元素图解; c—基性麻粒岩样品微量元素图解

图 9 不同变质级别样品中磷灰石微量元素图解

Fig. 9 Trace element diagram of apatite grains of different metamorphic grades

(a) Trace element diagram of apatite grains of greenschist; (b) Trace element diagram of apatite grains of plagioclase amphibolite; (c) Trace element diagram of apatite grains of mafic granulite

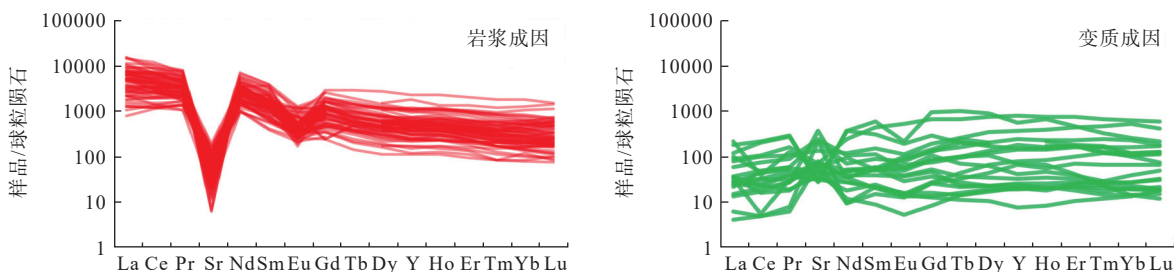


图 10 不同成因类型磷灰石微量元素图解 (据 O'Sullivan et al., 2020 修改)

Fig. 10 Trace element diagram of apatite of different genetic types (modified after O'Sullivan et al., 2020)

能为榍石和帘石族矿物等。与之相反, 基性麻粒岩样品 22WT-09 和 22WT-12 深熔成因磷灰石比全岩更富集 LREE, 表明深熔过程中其他富 LREE 副矿物分解释放的 LREE 可能被优先分配到磷灰石中。绿片岩样品全岩的 LREE 含量高于基性麻粒岩样品, 在这一变质阶段的岩浆成因磷灰石 LREE 含量也高于高级变质阶段基性麻粒岩样品的磷灰石, 这表明除了变质级别的变化之外, 磷灰石中 LREE 可能也

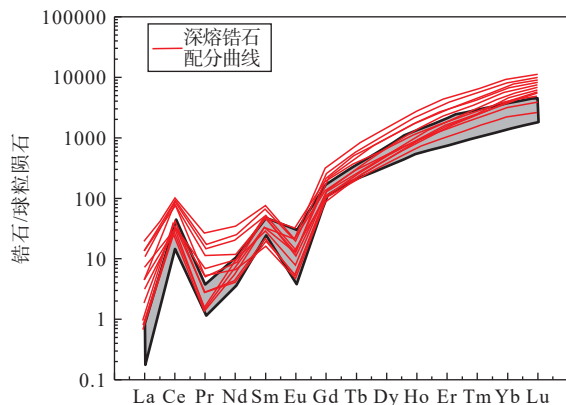
会在一定程度上受到全岩的影响。但此研究认为在高级变质阶段可能经历了深熔作用, 副矿物为深熔型矿物, 这意味着变质的影响是重要且不可避免的。

在进变质作用过程中, 随温压条件的升高以及变质流体的影响, 原岩中的造岩矿物会变得越来越不稳定, 从而分解形成新的变质矿物。已有研究表明, 在低—中级变质岩中岩浆成因和变质成因的磷灰石可能同时存在 (Henrichs et al., 2018)。文中的研

究结果也表明,在低级变质阶段,原岩中的岩浆成因磷灰石可以与经过变质作用新形成的变质成因磷灰石共存(图 9a)。随着温压条件的改变,共存比例中岩浆成因磷灰石的含量越来越低,不断转变为变质成因磷灰石,因此中级变质样品中几乎都是变质成因磷灰石,很少保留岩浆成因磷灰石。然而,高级变质阶段又重新出现具有岩浆成因特征的磷灰石,其 Sr 和 Eu 负异常程度相较于低级变质岩中的岩浆型磷灰石更为显著(图 9)。考虑到高级变质岩石普遍经历了广泛的深熔作用,笔者推测其中的磷灰石可能并非来自原岩的岩浆结晶,而是变质深熔过程中重结晶形成的。

这一现象与深熔锆石的成因有相似之处。岩浆型锆石可能在变质作用过程中形成变质型锆石,但经历深熔作用出现熔体后,之前不同成因的锆石会经过重结晶之后形成深熔型锆石(Chen and Zheng, 2017)。锆石的重结晶机制可分为固态转变、交代蚀变和溶解再沉淀(Xia et al., 2009, 2010; Chen et al., 2010, 2011),这 3 种机制主要取决于变质作用过程中流体和熔体影响的程度。就固态转变这一成因机制而言,深熔型锆石稀土元素模式保留了岩浆锆石的部分典型特征(图 11; Chen et al., 2010; Chen and Zheng, 2017; Xia et al., 2009)。

固态重结晶深熔型锆石可能在很大程度上保



灰色部分为岩浆成因的原岩锆石

图 11 大别-苏鲁造山带固态重结晶深熔锆石球粒陨石标准化稀土模式图(据 Chen and Zheng, 2017 修改; 文献数据参考 Chen et al., 2010; Xia et al., 2010)

Fig. 11 Chondrite-normalized REE patterns for solid-state recrystallization of metamorphosed zircons from the Dabie-Sulu Orogenic Belt (modified after Chen and Zheng, 2017; Reference data: Chen et al., 2010; Xia et al., 2010)

The gray zone denotes the protolith zircon of magmatic origin.

留了与岩浆型锆石相似的结构和地球化学特征。因此,笔者推测在高级变质阶段,深熔熔体的出现导致原来的副矿物(如不同类型的磷灰石)在熔体中重新结晶,形成深熔型磷灰石(图 9c)。其具有类似岩浆型磷灰石的微量元素特征,但并非真正的继承自原岩的岩浆成因磷灰石。

## 5 结论

通过对古元古代华北克拉通中部造山带五合一恒山地区不同变质级别变基性岩中的磷灰石进行了岩相学和主微量元素地球化学研究,对其成因类型进行区分,讨论其在变质演化过程的表现方式,结论如下:

(1)不同变质级别下变基性岩中磷灰石具有不同成因类型,主要体现在微量元素含量、稀土元素配分特征以及 Sr 异常程度上的差异。低级变基性岩中的磷灰石可区分为岩浆型和变质型 2 种,中级变基性岩中的磷灰石以变质型为特征,而高级变基性岩中的磷灰石只有深熔型,表现出岩浆型磷灰石的微量元素特征。

(2)岩浆型磷灰石在 CL 图中普遍呈半自形-自形,结构较为均一,微量元素呈现轻稀土富集以及 Sr、Eu 负异常的特征。变质型磷灰石在 CL 图中普遍呈半自形-他形,结构不均一,存在裂隙,微量元素呈现轻稀土亏损以及 Sr、Eu 正异常和负异常共存的特征。

(3)磷灰石在变质作用过程中的演变受到温压条件和深熔熔体的共同控制,同时还可能受到共生矿物的影响,主要与斜长石参与竞争 Sr,与楣石、帘石等参与竞争 LREE。随变质过程的进行,变质成因磷灰石逐渐增加,岩浆成因磷灰石减少;而到了高级变质作用的深熔阶段仅有深熔型磷灰石存在。岩浆型磷灰石中 Sr 负异常和变质型磷灰石 LREE 含量相对岩浆型磷灰石较低,分别体现了斜长石和楣石-帘石族矿物的影响。

## References

- BAI J, 1986. The Early Precambrian geology of Wutaishan[M]. Tianjin: Tianjin Science and Technology Press: 1-475. (in Chinese)
- BRUAND E, FOWLER M, STOREY C, et al., 2017. Apatite trace element and isotope applications to petrogenesis and provenance[J]. *American Mineralogist*, 102(1): 75-84.
- CHEN H X, LIU J H, ZHANG Q W L, et al., 2020. A long-lived tectono-

- metamorphic event in the Late Paleoproterozoic: evidence from SIMS U-Th-Pb dating of monazite from metapelite in central-south Trans-North China Orogen[J]. *Precambrian Research*, 336: 105497.
- CHEN R X, ZHENG Y F, XIE L W, 2010. Metamorphic growth and recrystallization of zircon: distinction by simultaneous in-situ analyses of trace elements, U-Th-Pb and Lu-Hf isotopes in zircons from eclogite-facies rocks in the Sulu Orogen[J]. *Lithos*, 114(1-2): 132-154.
- CHEN R X, ZHENG Y F, 2017. Metamorphic zirconology of continental subduction zones[J]. *Journal of Asian Earth Sciences*, 145: 149-176.
- CHEN W, SIMONETTI A, 2013. In-situ determination of major and trace elements in calcite and apatite, and U-Pb ages of apatite from the Oka carbonatite complex: insights into a complex crystallization history[J]. *Chemical Geology*, 353: 151-172.
- CHEN Y X, ZHENG Y F, CHEN R X, et al., 2011. Metamorphic growth and recrystallization of zircons in extremely  $^{18}\text{O}$ -depleted rocks during eclogite-facies metamorphism: evidence from U-Pb ages, trace elements, and O-Hf isotopes[J]. *Geochimica et Cosmochimica Acta*, 75(17): 4877-4898.
- CHEW D M, SPIKINGS R A, 2021. Apatite U-Pb thermochronology: a review[J]. *Minerals*, 11(10): 1095.
- CHU M F, WANG K L, GRILLFIN W L, et al., 2009. Apatite composition: tracing petrogenetic processes in Transhimalayan granitoids[J]. *Journal of Petrology*, 50(10): 1829-1855.
- FENG W Y, ZHENG J H, 2023. Apatite trace elements and O-Sr isotopes reveal different magmatic sources of Fe-Ti oxide deposits in the eastern Tianshan, NW China[J]. *Ore Geology Reviews*, 163: 105764.
- FILIPPELLI G M, 2002. The global phosphorus cycle[J]. *Reviews in Mineralogy and Geochemistry*, 48(1): 391-425.
- GALL Q, DAVIS W J, LOWE D G, et al., 2017. Diagenetic apatite character and in situ microprobe U-Pb age, Keeseville Formation, Potsdam Group, New York State[J]. *Canadian Journal of Earth Sciences*, 54(7): 785-797.
- GAO P, SANTOSH M, 2019. Building the Wutai arc: insights into the Archean-Paleoproterozoic crustal evolution of the North China Craton[J]. *Precambrian Research*, 333: 105429.
- GAO P, SANTOSH M, KWON S, et al., 2021. Ocean plate stratigraphy of a long-lived Precambrian subduction-accretion system: the Wutai complex, North China Craton[J]. *Precambrian Research*, 363: 106334.
- GAO S S, LI Q G, HU P Y, et al., 2023. Geochemical features and tectonic significance of Late Archean metavolcanic rocks in Hengshan Area, North China Craton[J]. *Acta Scientiarum Naturalium Universitatis Pekinensis*, 59(1): 143-160. (in Chinese with English abstract)
- GUO R R, LIU S W, SANTOSH M, et al., 2013. Geochemistry, zircon U-Pb geochronology and Lu-Hf isotopes of metavolcanics from eastern Hebei reveal Neoproterozoic subduction tectonics in the North China Craton[J]. *Gondwana Research*, 24(2): 664-686.
- GUO R R, LIU S W, WYMAN D, et al., 2015. Neoproterozoic subduction: a case study of arc volcanic rocks in Qinglong-Zhuzhangzi area of the eastern Hebei Province, North China Craton[J]. *Precambrian Research*, 264: 36-62.
- GUO R R, LIU S W, BAI X, et al., 2017. A Neoproterozoic subduction recorded by the eastern Hebei Precambrian basement, North China Craton: geochemical fingerprints from metavolcanic rocks of the Saheqiao-Shangying-Qinglong supracrustal belt[J]. *Journal of Asian Earth Sciences*, 135: 347-369.
- HAMMERLI J, GREBER N D, MARTIN L, et al., 2021. Tracing sulfur sources in the crust via SIMS measurements of sulfur isotopes in apatite[J]. *Chemical Geology*, 579: 120242.
- HE L C, ZHANG J, ZHAO G C, et al., 2021. Macro- and microstructural analysis of the Zhujiayang ductile shear zone, Hengshan complex: tectonic nature and geodynamic implications of the evolution of Trans-North China orogen[J]. *GSA Bulletin*, 133(5-6): 1237-1255.
- HENRICH S I A, O'SULLIVAN G, CHEW D M, et al., 2018. The trace element and U-Pb systematics of metamorphic apatite[J]. *Chemical Geology*, 483: 218-238.
- HOSKIN P W O, KINNY P D, WYBORN D, et al., 2000. Identifying accessory mineral saturation during differentiation in granitoid magmas: an integrated approach[J]. *Journal of Petrology*, 41(9): 1365-1396.
- HU Y L, LIU S W, FU J H, et al., 2021. Neoproterozoic-early Paleoproterozoic granitoids, the geothermal gradient and geodynamic evolution in the Hengshan Terrane, North China Craton[J]. *Gondwana Research*, 94: 143-163.
- HUGHES J M, RAKOVAN J F, 2015. Structurally robust, chemically diverse: apatite and apatite supergroup minerals[J]. *Elements*, 11(3): 165-170.
- KRÖNER A, WILDE S A, LI J H, et al., 2005a. Age and evolution of a Late Archean to Paleoproterozoic upper to lower crustal section in the Wutai/Hengshan/Fuping terrain of Northern China[J]. *Journal of Asian Earth Sciences*, 24(5): 577-595.
- KRÖNER A, WILDE S A, O'BRIEN P J, et al., 2005b. Field relationships, geochemistry, zircon ages and evolution of a Late Archean to Paleoproterozoic lower crustal section in the Hengshan Terrain of Northern China[J]. *Acta Geologica Sinica (English Edition)*, 79(5): 605-632.
- LI T S, ZHAI M G, PENG P, et al., 2010. Ca. 2.5 billion year old coeval ultramafic-mafic and syenitic dykes in Eastern Hebei: implications for Cratonization of the North China Craton[J]. *Precambrian Research*, 180(3-4): 143-155.
- LIU C H, LIU F L, SHI J R, et al., 2016a. Depositional age and provenance of the Wutai group: evidence from zircon U-Pb and Lu-Hf isotopes and whole-rock geochemistry[J]. *Precambrian Research*, 281: 269-290.
- LIU C H, ZHAO G C, LIU F L, et al., 2016b. Constraints of volcanic rocks of the Wutai complex (Shanxi Province, Northern China) on a giant Late Neoproterozoic intra-oceanic arc system in the Trans-North China Orogen[J]. *Journal of Asian Earth Sciences*, 123: 178-212.
- LIU J B, ZHANG L M, CHEN Y, et al., 2013. Chlorine contents in apatites of eclogites and hosted veins from the Dabie-Sulu UHP belt: implication for fluid evolution in the process of metamorphism[J]. *Chinese Science Bulletin*, 58(22): 2165-2168. (in Chinese with English abstract)
- LIU J H, ZHANG Q W L, LI Z M G, et al., 2020. Metamorphic evolution and U-Pb geochronology of metapelite, northeastern Wutai complex: implications for Paleoproterozoic tectonic evolution of the Trans-North China Orogen[J]. *Precambrian Research*, 350: 105928.
- LIU S Q, ZHANG G B, LI H J, 2023. Fingerprinting crustal anatexis with apatite trace element, halogen, and Sr isotope data[J]. *Geochimica et Cosmochimica Acta*, 351: 14-31.
- LIU S W, PAN Y M, LI J H, et al., 2002. Geological and isotopic geochemical constraints on the evolution of the Fuping complex, North China Craton[J]. *Precambrian Research*, 117(1-2): 41-56.

- LIU S W, PAN Y M, XIE Q L, et al., 2004. Archean geodynamics in the central zone, North China Craton: constraints from geochemistry of two contrasting series of granitoids in the Fuping and Wutai complexes[J]. *Precambrian Research*, 130(1-4): 229-249.
- LIU S W, ZHAO G C, WILDE S A, et al., 2006. Th-U-Pb monazite geochronology of the Lüliang and Wutai complexes: constraints on the tectonothermal evolution of the Trans-North China Orogen[J]. *Precambrian Research*, 148(3-4): 205-224.
- MAO M X, LIOU P, DU L L, et al., 2024. Petrogenesis of 2.7-2.65Ga TTGs in the Wutai complex: constraints on the Neoproterozoic crustal evolution of the North China Craton[J]. *Precambrian Research*, 400: 107245.
- MIYASHIRO A, 1974. Volcanic rock series in island arcs and active continental margins[J]. *American Journal of Science*, 274(4): 321-355.
- NATHWANI C L, LOADER M A, WILKINSON J J, et al., 2020. Multi-stage arc magma evolution recorded by apatite in volcanic rocks[J]. *Geology*, 48(4): 323-327.
- O'SULLIVAN G, CHEW D, KENNY G, et al., 2020. The trace element composition of apatite and its application to detrital provenance studies[J]. *Earth-Science Reviews*, 201: 103044.
- O'SULLIVAN G J, CHEW D M, 2020. The clastic record of a Wilson cycle: evidence from detrital apatite petrochronology of the Grampian-Taconic fore-arc[J]. *Earth and Planetary Science Letters*, 552: 116588.
- PAN L C, HU R Z, WANG X S, et al., 2016. Apatite trace element and halogen compositions as petrogenetic-metallogenic indicators: examples from four granite plutons in the Sanjiang Region, SW China[J]. *Lithos*, 254-255: 118-130.
- PATON C, HELSTROM J, PAUL B, et al., 2011. Iolite: freeware for the visualisation and processing of mass spectrometric data[J]. *Journal of Analytical Atomic Spectrometry*, 26(12): 2508-2518.
- PEARCE J A, 1996. A user's guide to basalt discrimination diagrams[M]//WYMAN D A. Trace element geochemistry of volcanic rocks: applications for massive sulphide exploration. St. John's: Geological Association of Canada: 79-113.
- PENG P, FENG L J, SUN F B, et al., 2017. Dating the Gaofan and Hutuo groups – Targets to investigate the Paleoproterozoic great oxidation event in North China[J]. *Journal of Asian Earth Sciences*, 138: 535-547.
- PICCOLI P M, CANDELA P A, 2002. Apatite in igneous systems[J]. *Reviews in Mineralogy and Geochemistry*, 48(1): 255-292.
- POLAT A, KUSKY T, LI J H, 2005. Geochemistry of Neoproterozoic (ca. 2.55-2.50 Ga) volcanic and ophiolitic rocks in the Wutaishan greenstone belt, central orogenic belt, North China Craton: implications for geodynamic setting and continental growth[J]. *GSA Bulletin*, 117(11-12): 1387-1399.
- QIAN J H, WEI C J, ZHOU X W, et al., 2013. Metamorphic P-T paths and new zircon U-Pb age data for garnet-mica schist from the Wutai group, North China Craton[J]. *Precambrian Research*, 233: 282-296.
- QIAN J H, WEI C J, 2016. P-T-t evolution of garnet amphibolites in the Wutai-Hengshan area, North China Craton: insights from phase equilibria and geochronology[J]. *Journal of Metamorphic Geology*, 34(5): 423-446.
- SPEAR F S, PYLE J M, 2002. Apatite, monazite, and xenotime in metamorphic rocks[J]. *Reviews in Mineralogy and Geochemistry*, 48(1): 293-335.
- STOKES T N, BROMILEY G D, POTTS N J, et al., 2019. The effect of melt composition and oxygen fugacity on manganese partitioning between apatite and silicate melt[J]. *Chemical Geology*, 506: 162-174.
- SUN D, LI Q G, LIU S W, et al., 2019. Neoproterozoic magmatic arc evolution in the Wutai-Hengshan-Fuping area, North China Craton: new perspectives from zircon U-Pb ages and Hf isotopic data[J]. *Precambrian Research*, 331: 105368.
- SUN J F, YANG J H, ZHANG J H, et al., 2021. Apatite geochemical and Sr-Nd isotopic insights into granitoid petrogenesis[J]. *Chemical Geology*, 566: 120104.
- SUN S S, MCDONOUGH W F, 1989. Chemical and isotopic systematics of oceanic basalts: implications for mantle composition and processes, in *Magmatism in the Ocean Basins*[J]. *Geological Society, London, Special Publications*, 42(1): 313-345.
- TAN H M R, HUANG X W, MENG Y M, et al., 2023. Multivariate statistical analysis of trace elements in apatite: discrimination of apatite with different origins[J]. *Ore Geology Reviews*, 153: 105269.
- TANG L, SANTOSH M, 2018. Neoproterozoic granite-greenstone belts and related ore mineralization in the North China Craton: an overview[J]. *Geoscience Frontiers*, 9(3): 751-768.
- TANG M, LEE C T A, JI W Q, et al., 2020. Crustal thickening and endogenic oxidation of magmatic sulfur[J]. *Science Advances*, 6(31): eaba6342.
- TRAP P, FAURE M, LIN W, et al., 2007. Late Paleoproterozoic (1900-1800 Ma) nappe stacking and polyphase deformation in the Hengshan-Wutaishan area: implications for the understanding of the Trans-North-China belt, North China Craton[J]. *Precambrian Research*, 156(1-2): 85-106.
- WAN Y S, DONG C Y, XIE H Q, et al., 2022. Huge growth of the Late Mesoarchean-Early Neoproterozoic (2.6~3.0 Ga) continental crust in the North China Craton: a review[J]. *Journal of Geomechanics*, 28(5): 866-906. (in Chinese with English abstract)
- WANG C L, ZHANG L C, LAN C Y, et al., 2014. Petrology and geochemistry of the Wangjiashuang banded iron formation and associated supracrustal rocks from the Wutai greenstone belt in the North China Craton: implications for their origin and tectonic setting[J]. *Precambrian Research*, 255: 603-626.
- WANG X P, PENG P, LI X B, 2023. Petrogenesis and geological implications of the ca. 2520Ma gabbroic intrusions in Wutai Mountain of the North China Craton[J]. *Acta Petrologica Sinica*, 39(3): 845-864. (in Chinese with English abstract)
- WANG Z H, WILDE S A, WANG K Y, et al., 2004. A MORB-arc basalt-Adakite association in the 2.5 Ga Wutai greenstone belt: Late Archean magmatism and crustal growth in the North China Craton[J]. *Precambrian Research*, 131(3-4): 323-343.
- WEBSTER J D, PICCOLI P M, 2015. Magmatic apatite: a powerful, yet deceptive, mineral[J]. *Elements*, 11(3): 177-182.
- WEI C J, 2018. Paleoproterozoic metamorphism and tectonic evolution in Wutai-Hengshan region, Trans-North China Orogen[J]. *Earth Science*, 43(1): 24-43. (in Chinese with English abstract)
- WILDE S A, CAWOOD P A, WANG K Y, et al., 2004. Determining Precambrian crustal evolution in China: a case-study from Wutaishan, Shanxi Province, demonstrating the application of precise SHRIMP U-Pb geochronology[J]. *Geological Society, London, Special Publications*, 226(1): 5-25.
- XIA Q X, ZHENG Y F, YUAN H L, et al., 2009. Contrasting Lu-Hf and U-Th-Pb isotope systematics between metamorphic growth and recrystallization of zircon from eclogite-facies metagranites in the Dabie Orogen, China[J]. *Lithos*, 112(3-4): 477-496.

- XIA Q X, ZHENG Y F, HU Z C, 2010. Trace elements in zircon and coexisting minerals from low-T/UHP metagranite in the Dabie Orogen: implications for action of supercritical fluid during continental subduction-zone metamorphism[J]. *Lithos*, 114(3-4): 385-412.
- XING K, SHU Q H, 2021. Applications of apatite in study of ore deposits: a review[J]. *Mineral Deposits*, 40(2): 189-205. (in Chinese with English abstract)
- YANG Q Y, SANTOSH M, 2015. Paleoproterozoic arc magmatism in the North China Craton: no Siderian global plate tectonic shutdown[J]. *Gondwana Research*, 28(1): 82-105.
- YANG Q Y, SANTOSH M, 2017. The building of an Archean microcontinent: evidence from the North China Craton[J]. *Gondwana Research*, 50: 3-37.
- ZAFAR T, REHMAN H U, MAHAR M A, et al., 2020. A critical review on petrogenetic, metallogenic and geodynamic implications of granitic rocks exposed in north and East China: new insights from apatite geochemistry[J]. *Journal of Geodynamics*, 136: 101723.
- ZHAI M G, GUO J H, LIU W J, 2005. Neoproterozoic to Paleoproterozoic continental evolution and tectonic history of the North China Craton: a review[J]. *Journal of Asian Earth Sciences*, 24(5): 547-561.
- ZHAI M G, SANTOSH M, 2011. The Early Precambrian odyssey of the North China Craton: a synoptic overview[J]. *Gondwana Research*, 20(1): 6-25.
- ZHAI M G, 2019. Tectonic evolution of the North China Craton[J]. *Journal of Geomechanics*, 25(5): 722-745. (in Chinese with English abstract)
- ZHAN Q Y, ZHU D C, WANG Q, et al., 2022. Partitioning behaviors of some key elements in apatite and their implications[J]. *Bulletin of Mineralogy, Petrology and Geochemistry*, 41(6): 1087-1099. (in Chinese with English abstract)
- ZHANG J, ZHAO G C, SUN M, et al., 2006. High-pressure mafic granulites in the Trans-North China Orogen: tectonic significance and age[J]. *Gondwana Research*, 9(3): 349-362.
- ZHANG J, ZHAO G C, LI S Z, et al., 2007. Deformation history of the Hengshan complex: implications for the tectonic evolution of the Trans-North China Orogen[J]. *Journal of Structural Geology*, 29(6): 933-949.
- ZHANG J, ZHAO G C, LI S Z, et al., 2012. Structural pattern of the Wutai complex and its constraints on the tectonic framework of the Trans-North China Orogen[J]. *Precambrian Research*, 222-223: 212-229.
- ZHANG J, ZHAO G C, SHEN W L, et al., 2015. Aeromagnetic study of the Hengshan-Wutai-Fuping region: unraveling a crustal profile of the Paleoproterozoic Trans-North China Orogen[J]. *Tectonophysics*, 662: 208-218.
- ZHANG S Y, YANG L Q, HE W Y, et al., 2021. Melt volatile budgets and magma evolution revealed by diverse apatite halogen and trace elements compositions: a case study at Pulang porphyry Cu-Au deposit, China[J]. *Ore Geology Reviews*, 139: 104509.
- ZHAO G C, WILDE S A, CAWOOD P A, et al., 1998. Thermal evolution of Archean basement rocks from the eastern part of the North China Craton and its bearing on tectonic setting[J]. *International Geology Review*, 40(8): 706-721.
- ZHAO G C, CAWOOD P A, WILDE S A, et al., 2000. Metamorphism of basement rocks in the central zone of the North China Craton: implications for Paleoproterozoic tectonic evolution[J]. *Precambrian Research*, 103(1-2): 55-88.
- ZHAO G C, WILDE S A, CAWOOD P A, et al., 2001. Archean blocks and their boundaries in the North China Craton: lithological, geochemical, structural and *P-T* path constraints and tectonic evolution[J]. *Precambrian Research*, 107(1-2): 45-73.
- ZHAO G C, SUN M, WILDE S A, et al., 2005. Late Archean to Paleoproterozoic evolution of the North China Craton: key issues revisited[J]. *Precambrian Research*, 136(2): 177-202.
- ZHAO G C, KRÖNER A, WILDE S A, et al., 2007. Lithotectonic elements and geological events in the Hengshan-Wutai-Fuping belt: a synthesis and implications for the evolution of the Trans-North China Orogen[J]. *Geological Magazine*, 144(5): 753-775.
- ZHAO G C, WILDE S A, GUO J H, et al., 2010. Single zircon grains record two Paleoproterozoic collisional events in the North China Craton[J]. *Precambrian Research*, 177(3-4): 266-276.
- ZHAO G C, CAWOOD P A, LI S Z, et al., 2012. Amalgamation of the North China Craton: key issues and discussion[J]. *Precambrian Research*, 222-223: 55-76.
- ZHAO Y F, HU J M, GONG W B, et al., 2019. Comparison of main characteristics of different Precambrian blocks in the Trans-North China Orogen[J]. *Acta Petrologica Sinica*, 35(7): 2259-2279. (in Chinese with English abstract)

## 附中文参考文献

- 白瑾, 1986. 五台山早前寒武纪地质[M]. 天津: 天津科学技术出版社: 1-475.
- 高山松, 李秋根, 胡鹏月, 等, 2023. 华北克拉通恒山地区晚太古代变质火山岩的地球化学特征及构造意义[J]. 北京大学学报(自然科学版), 59(1): 143-160.
- 刘景波, 张灵敏, 陈意, 等, 2013. 大别-苏鲁造山带超高压榴辉岩和脉体磷灰石含氯特征与变质流体演化[J]. 科学通报, 58(22): 2165-2168.
- 万渝生, 董春艳, 颜强, 等, 2022. 华北克拉通新太古代早期-中太古代晚期(2.6~3.0 Ga)巨量陆壳增生: 综述[J]. 地质力学学报, 28(5): 866-906.
- 王欣平, 彭澎, 李小兵, 2023. 华北克拉通五台山~2520 Ma 辉长岩侵入体的成因及其地质意义[J]. 岩石学报, 39(3): 845-864.
- 魏春景, 2018. 华北中部造山带五台-恒山地区古元古代变质作用与构造演化[J]. 地球科学, 43(1): 24-43.
- 邢凯, 舒启海, 2021. 磷灰石在矿床学研究中的应用[J]. 矿床地质, 40(2): 189-205.
- 翟明国, 2019. 华北克拉通构造演化[J]. 地质力学学报, 25(5): 722-745.
- 詹琼睿, 朱弟成, 王青, 等, 2022. 磷灰石中一些关键元素的分配行为及意义[J]. 矿物岩石地球化学通报, 41(6): 1087-1099.
- 赵远方, 胡健民, 公王斌, 等, 2019. 华北中部构造带不同前寒武纪地块主要特征对比研究[J]. 岩石学报, 35(7): 2259-2279.